HHS Public Access

Author manuscript

Cell Rep. Author manuscript; available in PMC 2025 May 15.

Published in final edited form as:

Cell Rep. 2025 April 22; 44(4): 115557. doi:10.1016/j.celrep.2025.115557.

Phenotypic heterogeneity defines B cell responses to repeated SARS-CoV-2 exposures through vaccination and infection

Lela Kardava[1], **James Lim**[2], **Clarisa M. Buckner**[1], **Felipe Lopes de Assis**[1], **Xiaozhen Zhang**[1], **Wei Wang**[1], **Mattie L. Melnyk**[1], **Omar El Merhebi**[1], **Krittin Trihemasava**[1], **I-Ting Teng**[3], **Robin Carroll**[3], **Yogita Jethmalani**[3], **Mike Castro**[3], **Bob C. Lin**[3], **Lauren H. Praiss**[1], **Catherine A. Seamon**[4], **Peter D. Kwong**[3,5], **Richard A. Koup**[3], **Leonid Serebryannyy**[3], **David C. Nickle**[2,6], **Tae-Wook Chun**[1], **Susan Moir**[1,7,*]

[1]Laboratory of Immunoregulation, National Institute of Allergy and Infectious Diseases (NIAID), National Institutes of Health (NIH), Bethesda, MD 20892, USA

[2]Monoceros Biosystems, San Diego, CA 29130, USA

[3]Vaccine Research Center, NIAID, NIH, Bethesda, MD 20892, USA

[4]Critical Care Medicine Department, Clinical Center, NIH, Bethesda, MD 20892, USA

[5]Aaron Diamond AIDS Research Center, Columbia University Vagelos College of Physicians and Surgeons, New York, NY 10032, USA

[6]Department of Global Health, University of Washington, Seattle, WA 98105, USA

[7]Lead contact

SUMMARY

Long-lived humoral memory is key to durable immunity against pathogens yet remains challenging to define due to heterogeneity among antigen-reactive B cells. We addressed this gap through longitudinal sampling over the course of severe acute respiratory syndrome coronavirus 2 (SARS-CoV-2) mRNA vaccinations with or without breakthrough infection. High-dimensional phenotypic profiling performed on ~72 million B cells showed that receptor-binding domain (RBD) reactivity was associated with five distinct immunoglobulin G (IgG) B cell populations. Two expressed the activation marker CD71, both correlated with neutralizing antibodies, yet the one lacking the memory marker CD27 was induced by vaccination and blunted by infection. Two were resting memory populations; one lacking CD73 arose early and contributed to cross-

*Correspondence: smoir@niaid.nih.gov.

AUTHOR CONTRIBUTIONS

L.K., C.M.B., J.L., D.C.N., T.-W.C., and S.M. designed the research and analysis parameters. L.K., C.M.B., X.Z., W.W., M.L.M., O.E.M., K.T., R.C., Y.J., M.C., B.C.L., R.A.K., L.S., T.-W.C., and S.M. performed and/or supervised the experiments. L.S., L.K., J.L., F.L.d.A., and D.C.N. analyzed the data. L.H.P. and C.A.S. oversaw clinical recruitment and/or medical aspects or assisted with sample collection. I-T.T. and P.D.K. provided critical reagents. L.K., J.L., D.C.N., T.-W.C., and S.M. designed the figures. L.K., J.L., D.C.N., and S.M. wrote the manuscript. All authors reviewed and edited the manuscript.

DECLARATION OF INTERESTS

The authors declare no competing interests.

SUPPLEMENTAL INFORMATION

Supplemental information can be found online at https://doi.org/10.1016/j.celrep.2025.115557.

reactivity; the other, expressing CD73, arose later and correlated with neutralizing antibodies. The fifth, a rare germinal center-like population, contributed to recall responses and was highly cross reactive. Overall, robust and distinct responses to booster vaccination overcame the superiority of hybrid immunity provided by breakthrough infection.

Graphical abstract

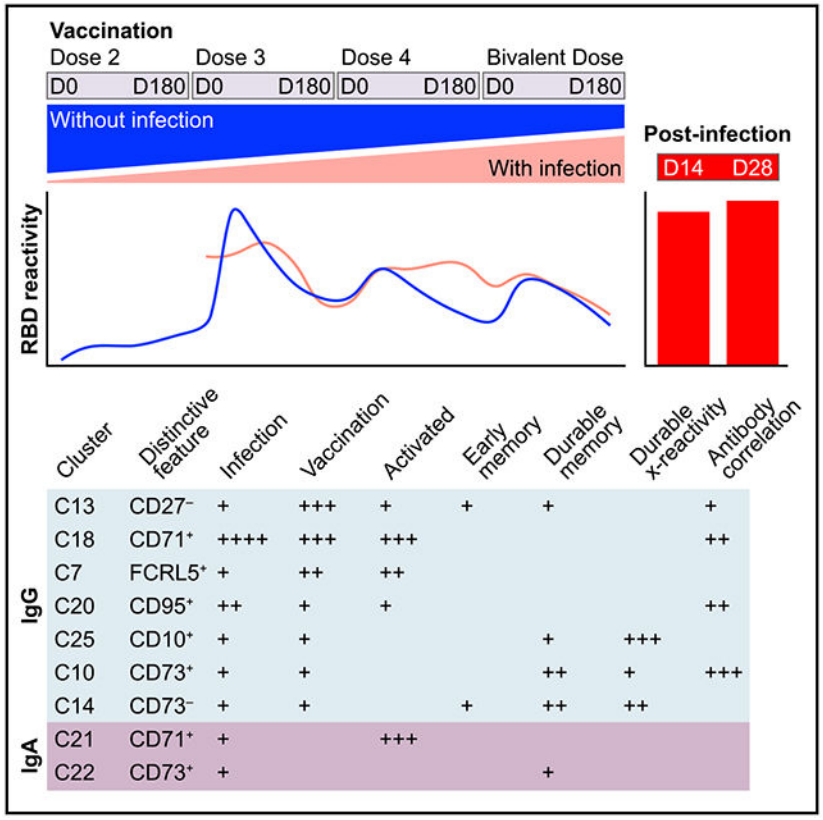

In brief

Phenotypes of pathogen-specific B cells elicited by repeated exposure remain unclear. Kardava et al. show that, without infection, the third dose of the COVID-19 mRNA vaccine elicited the strongest response, with phenotypes distinct from those of infection. Different phenotypes contributed to response induction/maintenance, cross-reactivity, and correlations with neutralizing antibodies.

INTRODUCTION

Severe acute respiratory syndrome coronavirus 2 (SARS-CoV-2) spike-encoding mRNA vaccines were developed shortly after the emergence of COVID-19 and shown to protect through the induction of potent neutralizing antibodies against the viral protein.[1–3] The primary two-dose mRNA vaccine was also found to elicit a robust and prolonged germinal center reaction that led to the establishment of a durable pool of memory B cells poised for rapid recall response upon re-exposure to SARS-CoV-2 (reviewed in Laidlaw and

Ellebedy[4]). However, while booster vaccination has also been shown to elicit robust antibody and cellular responses,[5–8] the effectiveness of boosters has been dampened by rapidly evolving antibody escape variants and a strong recall of the original immune response over that of emerging variants, an effect commonly known as immune imprinting.[9] Repeated exposure to SARS-CoV-2 infection and/or vaccination and the nature and timing of these exposure have also been shown to modulate humoral immunity against the virus.[10–16]

Antigen-experienced B cells are highly heterogeneous, expressing a wide range of cell-surface markers in addition to immunoglobulin isotypes that evolve and vary over time depending on the type and timing of antigenic exposure.[17,18] While a broad spectrum of distinct B cell populations has been described over the past decade, using advanced multiparametric approaches,[19,20] these had not been widely considered at the antigen-specific level until recently. The emergence of SARS-CoV-2 provided an unprecedented opportunity to follow the trajectory of antigen-specific B cells from initial priming through multiple exposures in the context of infection and vaccination. Early studies on B cell responses to SARS-CoV-2 infection identified plasmablasts and B cells with various profiles associated with activation that subsided over time to be replaced by populations of memory B cells with resting phenotypes.[21,22] With the availability of SARS-CoV-2 spike-based vaccines starting in late 2020, it became possible to extend these studies to include B cell responses to primary and secondary immunizations and begin to compare outcomes from different types of exposures. However, studies have reported both similarities and distinctions between responses to infection and vaccination,[23–27] and an increasing number of variables, such as differences in disease severity, timing between exposures, and the cross-sectional and increasingly mixed infection/vaccination nature of most cohorts, has added to difficulties in identifying clear outcomes.

Here, we delineated the effects of successive doses of SARS-CoV-2 mRNA vaccines and breakthrough infections on B cell and antibody responses in a longitudinal cohort first established in late 2020.[10,28] Our findings show that distinct populations of B cells responded to the vaccine, that these responses correlated with neutralizing antibody titers against the wild type and variants of SARS-CoV-2, and that these outcomes were modulated by repeated vaccinations and breakthrough infections.

RESULTS

Robust antibody responses to infection and booster vaccination without prior infection

We evaluated the longitudinal effects of multiple doses of the SARS-CoV-2 mRNA vaccine and breakthrough infections on antibody and B cell responses in a cohort of 33 study participants who received the first two doses of the Moderna mRNA-1273 vaccine, followed by one to three additional booster doses of either Moderna or Pfizer mRNA vaccines, the last being the ancestral (wild-type [WT])-BA.4/5 bivalent formulation (Table S1). Study time points began at baseline of dose 2, followed by post-vaccination days 14, 28, and 180 (month 6) and day 56 for the third and bivalent doses (Figure 1A). Time intervals between doses varied, with the shortest between doses 3 and 4 for the 10 participants who received a total of 5 doses during the study period (Table S1). Of the 33 participants, 11 remained

uninfected through the end of the study, confirmed by the absence of nucleocapsid (NC) antibodies (Figure 1B). Of the 21 participants who experienced a breakthrough infection during the study, 16 provided additional blood on post-infection day 14 and/or day 28 (Figure 1A; Table S1). At each vaccination time point, two categories were established, without infection (WOI) or with (WI) infection, depending on whether a participant remained uninfected or not at that time point. The number of participants per category at each time point ranged from 2 to 28 (Figure S1A). Of note, dose 2 (T1–T4) analyses were restricted to the non-infected category given that only one participant was infected prior to the baseline of dose 3 (Table S1).

First, we measured the binding of immunoglobulin G (IgG) antibodies to a panel of receptor-binding domain (RBD) of the spike proteins that included the WT and eight subsequent SARS-CoV-2 variants from Alpha through Omicron BA.5 (Figure 1B). IgG titers against all nine RBD proteins were significantly higher WI than WOI at baseline of dose 3 (T5); however, the response to dose 3 (slope T5–T6) was significantly stronger WOI than WI (Figure 1B). RBD IgG titers remained high through T18, with no significant differences in magnitude or slope between the two categories. IgA titers were lower but similar in pattern to those observed for IgG, except for increased titers at T14 WI and no difference in NC (Figure S1B). We then measured neutralizing antibodies against the WT, BA.5, and XBB.1.5 and found patterns similar to those of binding antibodies (Figure 1C). Neutralizing titers were significantly higher WI than WOI at T5, but the increase in titer following dose 3 was significantly greater WOI than WI for the WT and BA.5. Titers at T9 (BA.5) and T18 (XBB.1.5) were also higher WI than WOI (Figure 1C), although the difference for XBB.1.5 was driven by two participants who were infected close to T18 (Table S1; Figure S1C). Thus, consistent with previous reporting on a larger cohort,[29] antibody titers elicited by prior infection are superior to those of primary vaccination, although the effect is abrogated by a robust response to the first booster vaccine in the absence of infection, and responses to the subsequent booster do not differ by infection status.

B cell phenotypes associated with responses to SARS-CoV-2 vaccine and infection

To evaluate the B cells that responded to SARS-CoV-2 vaccination and infection, we performed spectral flow cytometry using a panel of antibodies against 26 cell-surface markers (Table S2) that was informed by recent multiparametric immunophenotyping of human B cell populations[19,20] and markers associated with reactivity to SARS-CoV-2.[21,27,28,30] From a total of 72 million $CD3^{-}CD45^{+}CD19^{+}$ cells gated from the peripheral blood mononuclear cells (PBMCs) of all participants and at all time points, we performed unsupervised clustering and dimensionality reduction with 23 markers, which generated 30 distinct B cell clusters (Figure 2A). Most B cells belonged to naive clusters, located near one another by uniform manifold approximation and projection (UMAP), with an immature/transitional cluster above, IgD/M unswitched memory and plasmablast (PB) clusters below, and a separate group of IgA/G switched memory and PB clusters near the bottom (Figure S2A; Table S3 for detailed annotations). CD10 is a marker that is expressed at two distinct stages of B cell development: from the pre-B to the immature/transitional stage and again during differentiation of germinal center B cells (GCBCs).[31,32] In the peripheral blood, most CD10-expressing B cells are $CD27^{-}$ and thus immature,[33] although a

small fraction co-expresses the differentiation marker CD27 (Figure S2B).[34] Among the 30 clusters, four distinctly expressed CD10: one immature/transitional cluster (cluster 5 [C5]) and three minor clusters distinguished by isotypes IgD/M (C8), IgG (C25), or IgA (C26). These three clusters express other GCBC markers (CD27, CD38, CD73, and CD11a),[35–37] suggesting that these may be circulating counterparts of GCBCs.

Five spike proteins were included in the staining panel: WT sub-unit 1 (S1), its constituent RBD and N-terminal domain (NTD), and RBD and NTD of BA.4/5, the variant in the 2022 bivalent vaccine. There was minimal binding of BA.4/5 in the absence of its WT counterparts, consistent with effects of imprinting.[38] Accordingly, the binding of RBD was measured from within the WT S1 gate and cells or clusters referred to as being RBD reactive for all RBD binding or cross-reactive for dual WT and BA.4/5 RBD binding (Figure S2C). We then determined RBD reactivity among the 30 B cell clusters, which generated a new map showing 27 clusters with RBD reactivity, dominated by IgG clusters (Figure 2B). Minor RBD reactivity was noted in PB C28, which was split into two areas, IgA and IgG, consistent with the composition of the cluster and detection of low-intensity cell-surface-expressed IgG PBs (Figure S2D), as reported previously.[28]

Next, we considered RBD reactivity among the 27 B cell clusters in response to infection by overlaying the map in Figure 2B with RBD reactivities on days 14 and 28 post infection for 11 and 16 samples, respectively, and contrasting them with their closest corresponding post-vaccination WOI time points (Table S1). Day 14 post exposure contained RBD-reactive clusters that were more activated and included more PBs than on day 28, and there were clear differences between responses to infection versus vaccination (Figure 2C). IgA clusters were more dominant after infection than vaccination, while for IgG, non-overlapping clusters were dominant, especially on day 28 post exposure. Next, we plotted the median contribution of each cluster to the total RBD response at each time point (Figure 2D). Among WOI time points, frequencies of RBD-reactive B cells increased modestly after vaccine dose 2 and remained stable through ~9 months (T5 was a median of 286 days between doses 2 and 3), consistent with previous findings.[28,39] These frequencies rose sharply after dose 3 (T6), driven by clusters with activated phenotypes, peaking on day 14, and were then replaced with more resting phenotypes as the total response diminished (see Table S3 for annotations). Similar patterns were observed with subsequent booster doses, albeit with less magnitude than observed after dose 3 (Figure 2D). Frequencies of RBD-reactive B cells on days 14 and 28 post infection were similar in magnitude to post-vaccination T6 WOI but not WI, consistent with previous findings.[10] Thus, while infection and the first booster vaccine without prior infection elicited similarly strong RBD reactivities, the B cell phenotypes elicited by each were distinct, and overall reactivities diminished with repeated exposures.

Distinct clusters of activated B cells contribute to responses to the first booster and infection

To further evaluate which B cell phenotypes contributed to the responses to vaccination and infection, we first focused on clusters at time points with the highest frequencies of RBD-reactive B cells (Figure 2D). To address vaccine dose effects, we compared peaks or

areas under the curve (AUC) of RBD reactivity within dose 3, which induced the strongest response WOI, to the peak or AUC of other vaccine doses. To address exposure effects (Figure 2C), we compared day 14 to day 28 reactivities post infection and between the two post-infection time points to their corresponding closest post-vaccination time point WOI. C18 is a cluster of IgG B cells expressing high levels of the activation markers CD71 and CD95, the memory markers CD27 and CD45RB, and near-normal levels of CD21 (Figure 2A), which was a major contributor to RBD reactivity at T6 WOI and post infection (Figure 2D). For time points WOI, the peak of dose 3 C18 RBD reactivity was significantly higher than peaks of all other doses (Figure 3A). C18 RBD reactivity was significantly higher on day 14 than on day 28 post infection, and significantly higher on days 14 and 28 post infection than corresponding post-vaccination time points (Figure 3A), consistent with recent findings.[15,40] The strong contribution of C18 to RBD reactivity post infection also explained the spikes at post-vaccination time points WI T9 and T17 (Figure 3A); these spikes at T9 and T17 were completely abrogated when participants with breakthrough infections close to these time points were excluded (Figure S3A). Similar effects were noted for two other clusters: C21, the IgA counterpart of C18, and C28, the predominantly IgA PB cluster (Figures 2A, S3B, and S3C). Both C21 and C28 RBD reactivities were strongly induced by infection alone and were significantly more elevated on day 14 than on day 28 post infection (Figures S3B and S3C).

IgG cluster C13 was another major contributor to RBD reactivity at T6 WOI but had a lesser role post infection (Figure 2D). Although C13 does not express the classic markers of memory CD27 and CD45RB, similar IgG-expressing populations have been described in the memory response to primary vaccination against influenza, SARS-CoV-2, and other pathogens.[10,41–44] C13 cells are $CD21^{+}CD38^{+}CD11c^{-}$, which contrasts with atypical memory cluster C17, and express the naive markers interleukin-4 receptor (IL-4R), CD23, and CD200 as well as the activation marker CD71 (Figure 2A), consistent with a previous report.[27] Peak C13 RBD reactivity WOI increased significantly from dose 2 to dose 3, and dose 3 C13 RBD reactivity was significantly higher WOI than WI by AUC and close by peak (false discovery rate [FDR] = 0.06; Figure 3B). In contrast to C18, C13 RBD reactivities rose modestly between days 14 and 28 post infection and were significantly lower on days 14 and 28 post infection than corresponding post-vaccination time points WOI (Figure 3B).

A third cluster, C7, while not a major contributor to overall RBD reactivity (Figure 2D), underwent distinct fluctuations in RBD reactivity following successive rounds of vaccination (Figure 3C). C7 is an IgG cluster of $CD21^{lo}$ B cells expressing high levels of FCRL5, an immunoregulatory molecule linked to effector B cells,[45] and intermediate levels of CD11c and CD71 (Figure 2A). C7 also expresses CD27 and low levels of CD45RB, which distinguishes it from the more atypical IgG memory cluster C17 (Figure 2A). Of note, C17 was a minor contributor to overall RBD reactivity (Figure 2D). Peak C7 RBD reactivity for dose 3 WOI was significantly higher than for doses 2 and 4 WOI and dose 3 WI (Figure 3C). C7 RBD reactivities were also significantly lower on days 14 and 28 post infection than corresponding post-vaccination time points WOI (Figure 3C). However, the diminutions in C7 RBD reactivity after the fourth and bivalent doses relative to dose 3 were significantly greater WOI than WI (Figure 3C). Thus, while infection alone did not

strongly induce C7 RBD reactivity, prior infection had an enhancing effect on the response to successive boosters that was otherwise progressively lost in the absence of infection. In contrast, infection alone strongly induced C18 RBD reactivity, more so than vaccination alone, although the response to dose 3 WOI was also robust. In contrast to both C7 and C18, C13 RBD reactivity was strongly induced by booster vaccination alone, more so than infection alone, and there was no benefit of prior infection on inducing or maintaining response to vaccination.

Different clusters after vaccination and infection contribute to the memory B cell response

Despite extensive heterogeneity among populations of memory B cells,[17,18] those that persist following self-resolving antigenic exposure tend to have common features associated with quiescence: expression of memory markers, CD27 and CD45RB, along with CD21 and minimal expression of activation markers.[17,46–48] The four largest non-naive B cell clusters were in this category: C2 (IgD/M), C22 (IgA), and two related IgG clusters, $CD73^+$ C10 and $CD73^-$ C14 (Figure 2A). C20, a minor intermediately activated ($CD95^+CD71^{lo}$) IgG cluster, was also included. C2 (IgD/M), while a minor contributor to overall RBD reactivity (Figure 2D), was significantly higher at T6 WI than WOI, although the response to infection alone was weak (Figure S4A), suggesting that prior infection had an additive albeit transient effect to the first booster vaccine.

C22 (IgA), while also a minor contributor to overall RBD reactivity, was significantly higher at T6 and T14 WI than WOI and on day 28 post infection compared to the corresponding post-vaccination time point WOI and to day 14 post infection (Figure 4A). IgG clusters C10 and C14 differed primarily by the expression of CD73, absent on C14 and strongly expressed on C10 (Figure 2A). At baseline (T5) and on day 14 (T6) of dose 3, C10 but not C14 RBD reactivities were significantly higher WI than WOI, reflecting a weak C10 response to dose 2 WOI (Figures 4B and 4C). Nonetheless, AUCs of RBD reactivity for both C10 and C14 WOI increased significantly between dose 2 and subsequent doses (Figures 4B and 4C). C20, the IgG cluster with low-grade activation, was also significantly higher WI than WOI at T5 (Figure 4D). Furthermore, RBD reactivities within these three IgG clusters significantly increased from day 14 to day 28 post infection and were significantly higher on day 28 post infection than the corresponding post-vaccination time point WOI (Figures 4B–4D). The post-infection patterns for these three IgG clusters mirror those of C22, the IgA counterpart of C10 (Figure 2A), and are consistent with the gradual transition after exposure from activated to resting memory phenotypes.

Most of the significant differences between WOI and WI were observed prior to or shortly after dose 3 (T5 and T6), when there were only four people in the WI category, indicating a strong effect of prior infection early on, although this finding needs to be confirmed with a larger cohort. However, there were no significant differences between WOI and WI on day 180 of dose 3, when the number of infected people had risen to 11, and for the last vaccine dose, when there were more infected than non-infected people (Figure S1A). Of note, when the same number of exposures were compared (namely, four vaccine doses WOI versus three WI), RBD reactivities among several clusters were significantly higher WI than WOI at baseline and at certain time points between days 14 and 56 but not day 180 (Figure S4B).

These included C18, the IgG-activated cluster strongly induced by infection, and three IgA clusters (C21, C22, and C26), consistent with stronger IgA responses to infection than to intramuscular vaccination.[49] Thus, while infection led to superior responses among certain clusters, differences were no longer significant between WI and WOI by the last time point of dose 3 or when comparing the same number of exposures.

GCBC-like clusters are at the root of two distinct trajectories

GCBC-like clusters C8 (IgD/M), C25 (IgG), and C26 (IgA) collectively accounted for less than 2% of all B cells (Figure 2A). However, C25, and, to a lesser extent C26, were enriched among RBD-reactive cells, consistent with previous reporting,[30] and C25 was clearly discernable at most post-vaccination and post-infection time points (Figure 2D). C25 RBD reactivity was significantly higher at T6 WI than WOI, driven by a transient decrease post vaccination that was more pronounced without prior infection (Figure 5A). C25 RBD reactivity significantly increased from day 14 to day 28 post infection and was slightly higher on day 28 post infection than the corresponding post-vaccination time point WOI (Figure 5A). IgA GCBC-like cluster C26, while low in overall RBD reactivity (Figure S5A), was one of only three clusters where the effect of prior infection extended to the bivalent dose. For these analyses, we excluded the four individuals who were infected after receiving their bivalent vaccine, leaving a median interval of 169 days between the time of infection and vaccination for the remaining 13 individuals (Table S1). The peak and AUC of RBD reactivity following the bivalent dose were significantly higher WI than WOI among the two IgA clusters, resting memory C22 and GCBC-like C26, and significantly lower for the early memory (IgG^+CD27^-) cluster C13 (Figure 5B). These findings suggest that prior infection has a lasting effect on vaccine response.

We performed B cell trajectory analyses to learn more about temporal relationships between GCBC-like and other B cell populations. First, we established the positional relationships between clusters by projecting RBD-reactive B cells from all participants and all time points on 2-dimensional plots using the potential of heat diffusion for affinity-based transition embedding (PHATE) algorithm[50] (Figure 5C). We then traced pseudo-temporal relationships between clusters with the Wishbone algorithm,[51] using the unswitched memory B cell cluster C2 as the root, based on its RBD reactivity among IgD/M clusters and its positioning in the PHATE map. The trunk, comprised of all IgD/M and four core IgG clusters (GCBC-like C25, quiescent memory C10 and C14, and $CD27^-CD45RB^-$ C13; Figure S5B), bifurcated into two major branches, one containing IgG and the other IgA clusters (Figure 5C). Notably, the four core IgG clusters also contributed to both branches, with the two GCBC-like clusters C25 (IgG) and C26 (IgA) positioned at the base of each branch (Figure S5B). Sub-branches contained more activated/atypical clusters: C7, C17, and C18 in the IgG branch and C21 and C27 in the IgA branch (Figure 5C). C28, comprised mainly of IgA but also IgG PBs (Figure S2D), was found at the tips of the two branches, in closest proximity to C18 (IgG) and C21 (IgA), two related activated clusters (Figures 5C and 2A for phenotypes).

Having established the overall positional and pseudo-temporal relationships between RBD-reactive clusters, we then separately evaluated vaccine doses and infection status. WOI,

RBD reactivity to dose 3 (T5–T9) was dominated by all IgG clusters, contrasting with relatively more IgD/M clusters to the previous dose (T1–T4) and fewer activated IgG clusters to the last dose (T14–T18) (Figure 5D). WI, patterns were intermediate for T5–T9 and T14–T18, while post infection, days 14 and 28 had the fewest IgD/M clusters, and day 14 had more activated and PB clusters than day 28 post infection (Figure S5C). These patterns are consistent with cluster dynamics in Figures 2C and 2D. Last, we used dose 3 (T5–T9) WOI to evaluate real-time relationships after the two priming doses. As shown by overlay (Figure 5E), and for each time point separately (Figure S5D), baseline (T5) was populated by IgD/M and core IgG clusters, which then gave rise to more activated clusters at T6–T7 before being gradually replaced by more quiescent clusters through T8–T9 (month 6 post vaccination). Thus, these analyses identify GCBC-like B cell clusters C25 and C26 as potential sources of IgG and IgA responses and IgG core clusters C25, C10, C14, and C13 as contributing to the initiation and culmination of B cell responses following post-priming exposures in the absence of prior infection.

Cross-reactivity increases with the frequency but not the type of exposure

We considered temporal changes in cross-reactivity among the neutralizing antibody and B cell responses by comparing the fold WT or total over variant reactivities at the same time point following each dose (excluding dose 4 and day 56 time points and without considering prior infection). For neutralization antibody titers, fold WT over BA.5 decreased significantly from dose 2 to the bivalent dose on day 14 and day 28 time points and on day 180 between the third and bivalent dose (Figure 6A). Day 180 post dose 2 was not considered because too many BA.5 titers were below the limit of detection (Figure 1C), which artificially increased fold differences relative to later doses. After excluding all XBB.1.5 dose 2 time points for the same reason, we found the same significant decreases in fold neutralization titers of WT over XBB.1.5 as for BA.5 (Figure S6A), with no difference in fold differences between BA.5 and XBB.1.5 (Figure S6B). This suggests that the effect of successive vaccine doses was an overall increase in cross-reactivity and not a targeted effect of BA.4/5 in the bivalent vaccine, which is consistent with previous findings.[16,52,53] An enhancing effect of prior infection on vaccine-induced cross-reactivity was noted at the last time point, T18, although the difference was not significant for BA.5 when post-bivalent vaccine breakthrough infections were excluded (Figure S6C).

For B cells, we first evaluated differences in the proportion of $WT^{+}BA.4/5^{+}$ RBD cross-reactivity among all RBD-reactive B cells. The frequency of RBD cross-reactive B cells (all clusters combined) increased significantly from one vaccine dose to another, except on day 180 between doses 2 and 3 (Figure 6B). Vaccine-induced B cell cross-reactivity at the last time point, T18, was enhanced by prior infection, although the difference was not significant when post-bivalent vaccine breakthrough infections were excluded (Figure S6D). We then evaluated B cell clusters that contributed to the increasing overall RBD cross-reactivity, an analysis that was only meaningful for clusters and time points with substantial reactivities (Figure 2D). On days 14 and 28 post vaccination, when IgG clusters C7, C18, and C13 were the main contributors to RBD reactivity, the significant increases in RBD cross-reactivity from one dose to another were restricted to C7 and C18 (Figures 6C and S6E). On day 180 post vaccination, IgG memory clusters C10 and C14 were the main contributors to

overall RBD reactivity, and both displayed significant increases in RBD cross-reactivity between the last two doses, but only C10 was also significantly more cross-reactive when compared to dose 2 (Figure 6D). Finally, RBD reactivity within GCBC-like cluster C25, while too low for analysis at T4, displayed high cross-reactivity at T5 (baseline of dose 3) and no significant increase compared to T9 and T18 (Figure 6D). When comparing RBD cross-reactivities on day 180 between C25, C10, and C14, they were significantly higher in C25 than in C14 and C10 and significantly higher in C14 than in C10 at both T9 and T18 (Figure S6F). Thus, incremental increases in RBD cross-reactivities on days 14 and 28 were driven by activated clusters C7 and C18, those on day 180 by memory clusters C10 and C14, while GCBC-like cluster C25 was highly cross-reactive at all time points.

RBD reactivity among several B cell clusters correlates with neutralizing antibodies

Finally, we considered the association between RBD reactivity among B cell clusters and neutralizing antibody titers against WT, BA.5, and XBB.1.5. First, without considering infection status, we found strong and significant direct correlations between several RBD-reactive clusters and 50% inhibitory dilution (ID_{50}) and/or 80% inhibitory dilution (ID_{80}) titers against the three viruses, and most were concentrated at four time points following the first booster vaccine (dose 3): T7–T9 (days 28, 56, and 180) and T14, the baseline of the bivalent dose (Figure 7A). IgG CD73-expressing memory cluster C10, but not its CD73-negative counterpart C14, strongly correlated with neutralizing titers at all four time points and against all three viruses. C10 correlations were observed as early as T7 and as late as T18. Similar albeit less extensive patterns were observed for C20, the IgG memory cluster with a low-grade activation profile, and C18, the IgG activated cluster expressing high levels of CD71 (Figure 2A). Correlations were also observed at T9 and T14 for C21, the IgA counterpart of C18 (Figure 7A). These correlations were primarily driven by vaccination WOI (Figure S7A), although the lack of correlations at T7 and T8 WI may have been due to low numbers at these time points (Figure S1A). Most correlations were stronger when all datapoints were included, except for C13, the IgG early memory cluster, which had stronger, more extensive correlations when WI datapoints were excluded (Figure S7A). Last, we considered whether B cell responses at peak day 14 post-vaccination time points T6 and T15 were predictive of neutralizing antibody titers at day 180 post-vaccination time points T9 or T18. WOI, RBD reactivity in cluster C18 at T6 was strongly correlated with antibody titers at T9, and a similar pattern, although not quite as extensive, was observed for C13 and the naive cluster C1 (Figure 7B). C10 and C20 at T6 and T15 also correlated with antibody titers at respective day 180 time points, T9 and T18, although these were stronger without considering infection status (Figure 7C). WI, there were no significant correlations between early RBD-reactive clusters at later antibody titers (Figure S7B) despite an equal or greater number of individuals with than without prior infection from T15 to T18 (Figure S1A). Collectively, these data highlight the strong association between IgG clusters with activated (C18 and C20), early (C13), and quiescent (C10) memory phenotypes and neutralizing antibodies both at concurrent but also at later time points, thus suggesting that these populations may be drivers of humoral immunity.

DISCUSSION

The highly heterogeneous nature of antigen-experienced B cells in humans has made it difficult to identify phenotypes that are critical for generating and maintaining effective humoral memory. Through longitudinal sampling over several rounds of SARS-CoV-2 mRNA vaccination WI and WOI, we identified several distinct exposure-dependent phenotypes that contributed to the B cell and antibody responses to the virus. Core contributors were four IgG clusters: $CD27^{lo}$ C13, quiescent memory C10 ($CD73^{+}$) and C14 ($CD73^{-}$), and GCBC-like C25. RBD reactivities in C10 and C13 also strongly correlated with neutralizing antibody titers, with C13 correlations being strongest in the absence of infection, consistent with the minimal C13 RBD reactivity induced by or with infection. The role of CD73 in B cell memory has not been well defined.[17] Here, we show that C14, which lacks CD73, contributed to RBD reactivity earlier and with greater cross-reactivity than its $CD73^{hi}$ counterpart C10, while C10 RBD reactivity was more strongly associated with the neutralizing antibody response and more strongly induced by infection than vaccination alone. Thus, both C10 and C14, along with the other core contributors to RBD reactivity identified here, may contribute to the functional diversity thought to be critical for generating long-lived protective immunity.[4,17,46,54–56] Of note, functional longevity of anti-smallpox memory B cells in the spleen and circulation has been attributed to IgG^{+} B cells with phenotypic features similar to C10 ($CD73^{+}CD21^{+}CD27^{+}$).[57] The spleen has also been shown to harbor SARS-CoV-2 spike-reactive B cells,[58] although frequent re-exposures limit assessment of longevity. The functional importance of vaccine-induced memory B cells in protecting against symptomatic SARS-CoV-2 was recently established in children,[59] where $CD21^{+}CD27^{+}$ B cells have been shown to dominate responses within a few months of exposure.[60]

The unsupervised clustering performed on 72 million B cells provided a unique opportunity to identify minor populations with potentially important roles. Among minor populations were three $CD10^{+}$ $CD27^{+}$ clusters with GCBC-like features,[30,31,33,34] which collectively represented less than 2% of the total count, yet two, IgG C25 and IgA C26, contributed substantively to RBD reactivity. Pseudo-temporal PHATE mapping placed the GCBC-like clusters at the root of their respective IgG and IgA branches, and real-time mapping identified IgG C25 as both initiating and sustaining recall responses. C25 also contributed to RBD reactivity post infection and C26 to RBD reactivity post vaccination with prior infection. Furthermore, and consistent with a germinal center (GC) origin, the noticeable transient decreases in RBD-reactive C25 at the peak of overall RBD reactivities (day 14 post vaccination) may have been from migration into lymphoid tissues and the high RBD cross-reactivity in C25 from prolonged affinity maturation in the GC, as reported for SARS-CoV-2 mRNA vaccines.[61] Notably, low expression of CD95, a strong mediator of GCBC death by apoptosis,[62] was observed here on GCBC-like clusters and previously by single-cell transcriptomics,[30] and may provide a survival advantage outside lymphoid tissues.

Among the 30 clusters identified, about a third had an activated phenotype, although only a few of these contributed to RBD reactivity. IgG cluster C18 was a major contributor to day 14 peak reactivity after the first booster vaccine without prior infection and after infection. C18 cells express high levels of CD71, an early marker of B cell activation.[63]

C18 RBD reactivity also correlated strongly with neutralizing antibodies across multiple time points. Notably, its peak (day 14) RBD reactivity after the first booster without prior infection correlated with day 180 neutralizing antibodies, suggesting that C18 reactivity is a predictor of sustained neutralizing antibody titers, which, in turn, predicts vaccine efficacy.[64] The importance of C18, and, to a lesser extent, C7, which also showed strong RBD reactivity after the first booster vaccine without prior infection, was in stark contrast to C17, an IgG cluster with an atypical phenotype observed across several chronic infectious and inflammatory conditions.[65] Features of C7, an amalgam of C18 and C17, included expression of CD27 and FCRL5 yet relatively low CD11c and CD21, were most consistent with effector B cells elicited by influenza vaccines[45] and activated memory B cells in HIV infection.[66] It is noteworthy that C17, while dominant in chronic/inflammatory diseases, was a minor contributor to RBD reactivity following SARS-CoV-2 vaccination/infection, and its RBD reactivity did not correlate with neutralizing antibody titers, consistent with previous findings.[28]

Studies have reported additive immunological benefits from vaccination and infection, known as hybrid immunity,[23,67] although the underlying drivers remain largely undefined. Certain RBD-reactive clusters were more strongly induced by infection than vaccination alone, such as activated IgG clusters C18 and C20, which, like C18, strongly correlated with neutralizing antibodies at both concurrent and non-concurrent time points. Conversely, RBD reactivities in activated IgG clusters C7 and C13 were more strongly induced by vaccination than infection alone, although reactivity in C7 was also more strongly diminished by successive vaccine doses without than with prior infection. It is noteworthy that post-vaccination RBD reactivity in C13 was restricted by prior infection, consistent with our previous findings,[10] an effect that persisted through the last vaccine dose. B cells with a C13 phenotype (IgG^+CD27^-) have been shown to contribute to lasting primary immunity in several different settings.[10,41–44] Here, we show their importance to secondary immunity, both in the induction and culmination of the recall response and as correlates of neutralizing antibodies.

Last, while RBD reactivities in certain clusters—namely memory clusters C22 (IgA) and C10 (IgG) and pauci-activated C20 (IgG)—were stronger with than without prior infection after the first two doses of vaccine, the differences did not persist. However, we cannot exclude that differences may persist among tissue-resident B cells or antibodies. Spike-specific IgA in nasal mucosa have been shown to provide cross-variant protection[68] and are more strongly induced by infection than by intramuscular vaccines such as SARS-CoV-2.[49] We found relatively high cross-reactivity among several clusters that increased with vaccine doses, consistent with other recent findings,[16] and with inherent differences between memory B cells and plasma cells.[69] A paucity of antibodies at the site of exposure and the time needed for the cross-reactive B cells to differentiate into antibody-secreting cells may help explain why breakthrough infections are common but less severe with vaccination.[46] Overall and despite some caveats, our findings suggest that, while qualitative differences in RBD reactivity may persist between types of exposure, repeated exposures through infection and/or vaccination led to similar outcomes that were driven by a handful of distinct B cell populations. Our results can thus provide a road-map for evaluating the outcomes of different vaccines against SARS-CoV-2 or other pathogens.

Limitations of the study

The primary limitation of our study was the relatively small number of participants in each category that may have precluded discovery of additional significant differences to those reported. The small number of participants also precluded evaluating differences associated with demographics such as sex, age, and race. This was an observational study, and, as such, we could not control variables such as which mRNA vaccine the participants received, time interval between infection and post-vaccination visits, or the number of and time interval between vaccinations or availability for all study visits. While we found that IgG was the main contributor to antibody and B cell responses through repeated and varied exposures, we did not determine whether this led to more switching to IgG4, as others have shown.[70–72] We did not determine whether differences in the levels of RBD cross-reactivity among clusters reflected differences in affinity maturation, and we did not formally link GCBC-like clusters to GCBC in lymphoid tissues. This warrants follow-up studies with sufficient cells to address differences and properties at the single-cell level.

STAR★METHODS

EXPERIMENTAL MODEL AND STUDY PARTICIPANT DETAILS

Ethics statement: Participants were initially enrolled in a general phlebotomy blood draw protocol (ClinicalTrials.gov identifier NCT00001281) and later in the Vaccine Responses to SARS-CoV-2 and Other Emerging Infectious Diseases (COVAC) study (ClinicalTrials.gov identifier NCT05078905) at the NIH Clinical Center. The protocols were approved by the NIH Institutional Review Board and written informed consent was obtained from all study participants.

HUMAN STUDY SUBJECT RECRUITMENT, VISITS, AND CLINICAL DATA

A total of 33 adults were recruited and received a minimum of three doses of the Pfizer (BNT162b2) or Moderna (mRNA-1273) mRNA vaccine, 25 on whom we had samples collected during the primary immunization period (doses 1 and 2). The median age was 54 (range 22–65) years, 20 were female (61%), and 24 were white (73%). Details of demographics, including dates of vaccination, infection and blood donations pre-vaccination and post-vaccination/infection are provided and summarized in Table S1. One subject had COVID-19 prior to the first dose and another 21 over the course of the study, while 11 remained non-infected throughout the study period which began at the baseline of dose 2 and extended through 180 days after the 2022 bivalent vaccine dose. At each vaccination time point, participants were divided into one of two categories, depending on whether infection with SARS-CoV-2 had occurred by that time point. Several participants also donated blood after being diagnosed with COVID-19 and confirmed by the presence of nucleocapsid antibodies. Blood was collected up to a maximum of 20 time points per participant, depending on the total number of vaccine doses received and whether the participant returned after a breakthrough infection (Table S1). For six participants, day 180 after dose 3 (T9) coincided with the baseline of dose 4 (T10), and in three participants, COV_003, COV_015 and COV_101, a post-infection coincided with a post-vaccination time point (Table S1). The number of exposures for each participant at each timepoint was

calculated by summing the total number of infections and vaccine doses recorded up to that time point, based on the dates of exposure and the corresponding blood draw time points.

METHOD DETAILS

Blood sample collection, processing, and storage: PBMCs were isolated by Ficoll density gradient centrifugation from whole blood collected in ethylenediaminetetraacetic acid Vacutainer tubes. Cells were frozen at −80°C and stored in liquid nitrogen. Serum was isolated by centrifugation of clotted whole blood collected in serum separation transport Vacutainer tubes and stored at −80°C.

Serum antibody binding and neutralization assays: Serum samples were heat-inactivated at 56°C for 60 min. A 10-plex IgG spike-binding assay was performed with an electrochemi-luminescence immunoassay analyzer (ECLIA) developed by Meso Scale Discovery (MSD), as previously described,[10] with the following modification. The assays were performed using the MSD V-PLEX SARS-CoV-2 key variant RBD panel 1 for IgG and IgA detection. SARS-CoV-2 neutralization was performed with a lentiviral pseudovirus-based assay on heat-inactivated serum samples, as previously described.[77] Samples were tested in duplicate with eight dilutions per sample and neutralization curves were fitted through the averaged replicates at each dilution. The data were reported as reciprocal 50% or 80% inhibitory dilution (ID_{50} or ID_{80}) with a value of 20 plotted for samples that did not neutralize. Antibody binding arbitrary units (a.u./mL) and neutralization assay values were log2 transformed for analysis.

Flow cytometric analysis: A 31-color panel was developed to phenotype B cells and measure their SARS-CoV-2 reactivity by spectral flow cytometry (key resources table for list and source of antibodies and biotinylated spike proteins). Biotinylated spike proteins were tetramerized with fluorescently labeled streptavidin (SA) at a molar ratio of 4:1 as described previously,[10,28] with the following modifications: WT S1 was conjugated with SA-R-Phycoerythrin (PE), WT RBD with SA-BV421, BA.4/5 RBD with SA-Alexa Fluor 488, WT NTD with SA-BUV737 and BA.4/5 NTD with SA-BUV615. Cryopreserved PBMCs were thawed, and 3×10^6 cells were stained with Zombie NIR Fixable Viability Dye at room temperature for 10 min followed by staining with a cocktail containing 25 monoclonal antibodies (mAbs) and 5 fluorochrome-conjugated spike proteins in staining buffer (2% FBS/PBS) supplemented with Super Bright Complete Staining Buffer and CellBlox Blocking Buffer (ThermoFisher) at 4°C for 30 min. After staining, the cells were fixed with BD FACS Lysing Solution (BD Biosciences) and acquired on an Aurora spectral cytometer using SpectroFlo Software v3.2.1 (Cytek Biosciences) and analyzed using FlowJo v10.10 (BD Biosciences). FCS files from gated single, live $CD45^+CD3^-CD19^+$ B cells were exported from all participants at all time points for downstream analysis.

FlowSOM clustering and UMAP embedding: FlowSOM clustering and UMAP embedding were performed on exported FCS files using the OMIQ platform (omiq.ai). FlowAI algorithm was used to clean FCS data of undesired events. The following markers were used to perform FlowSOM clustering on a total of 72 million $CD19^+$ cells: CD19, CD20, CD10, CD38, CD27, CD21, CD71, CD11c, FCRL5, CXCR3, CD95, CD11a,

CD45RB, CD39, CD29, CD73, IL-4R, CD23, CD200, IgD, IgM, IgG, IgA, with the number of desired clusters set to 30 that was confirmed using the Elbow metaclustering algorithm in OMIQ. To visualize the clusters in a UMAP embedding, 2 million cells were subsampled from 72 million B cells to include 4,192 cells per sample from the 33 longitudinal participants at all time points. Additionally, UMAP projection of clusters was performed on RBD-reactive B cells defined by gating on WT $RBD^+/S1^+$ B cells from all study participants at all time points. The raw data generated by FlowSOM clustering were exported as a CSV file from OMIQ for further analysis.

The percentage of RBD^+ cells (RBD reactivity) within each cluster was normalized relative to the total number of B cells acquired in the sample. This was calculated by dividing the RBD^+ cell-count in each cluster by the total count of live $CD45^+CD3^-CD19^+$ cells and multiplying by 100. The slope of the percent RBD reactivity within clusters of interest between successive time points was calculated by subtracting the percentage at the earlier time point from the percentage at the later timepoint. $WT^+BA.4/5^+$ cross-reactivity among total B cells or selected clusters was calculated as the proportion of $WT^+BA.4/5^+$ among WT $RBD^+/S1^+$ counts and excluded data with a count of zero.

Trajectory analysis: Wishbone algorithm in OMIQ was used to perform trajectory analysis and pseudotime inference of RBD-reactive B cells. To perform Wishbone, RBD-reactive B cells from all participants at all time points and clusters defined by FlowSOM were first subjected to PHATE to project the data in 2 dimensions. Next, diffusion maps were generated to identify the major trend in the data as a part of trajectory analysis. The unswitched memory B cell cluster C2 was set as the root. Wishbone ordered the cells according to their progress through the developmental program and the pseudotime values were projected on PHATE plots to infer cellular relationships along trajectory.

QUANTIFICATION AND STATISTICAL ANALYSIS

The data processing methods used are described in respective sections of the Methods and specific statistical details are indicated in respective Figure legends. These details include the type of statistical test used, whether mean or median is depicted in Figure graphs, and an explanation of *p* or FDR values depicted in Figure panels.

Non-paired comparisons were performed using the Mann-Whitney test, and paired comparisons were conducted using the Wilcoxon signed-rank test (paired Wilcoxon test; wilcox.test() function), followed by the Benjamini-Hochberg method to control the false discovery rate or to adjust *p* values for multiple testing (p.adjust() function, R stats package v4.3.3).

Comparisons of the distribution of slope differences between infected and non-infected status were performed using the exact Fisher-Pitman permutation tests with the oneway_test() function from the R coin package (v1.4–2).[78] To compare RBD reactivities within each dose-time block, the peak percentage of cells in the clusters of interest was identified, and the AUC for these percentages was calculated. A general linear model (GLM) using Beta regression (betareg function from the betareg R package, v3.1–4) modeled the AUC or peak percentage of cells as a function of the interaction between dose-time block

and infection status.[79,80] Alternatively, data split by infection status was modeled as a function of the dose-time block. *p* values were obtained from the model using a likelihood ratio test.

Spearman correlation assessed the relationship between variables. Correlation heatmaps were generated using the geom_tile() function (ggplot2 package v3.5.0). The function −log10(*p*_value)/max(−log10(*p*_value))*0.9 normalizes and scales the data, restricting the range to [0, 0.9]. This transformation determines the tile size in the heatmap with higher values indicating greater significance. Data wrangling utilized the dplyr (v1.1.4) and tidyverse (v2.0.0) packages. Data visualization was performed with ggplot2 (v3.4.2), gridExtra (v2.3), and scales (v1.3.0).

Supplementary Material

Refer to Web version on PubMed Central for supplementary material.

ACKNOWLEDGMENTS

We thank all participants for their willingness to take part in this study and Catherine Rehm, Ulisses Santamaria, Jessica Earhart, Bryan Higgins, Kathleen Gittens, Ali Rai, and Michael Sneller for clinical support. This work was funded by the Intramural Research Program of the Division of Intramural Research of NIAID, NIH, and the Vaccine Research Center, an intramural Division of NIAID, NIH.

RESOURCE AVAILABILITY

Lead contact

Requests for further information, resources, and reagents should be directed to and will be fulfilled by the lead contact, Susan Moir (smoir@niaid.nih.gov).

Materials availability

This study did not generate new unique reagents.

Data and code availability

- All raw data in this paper are publicly available as of the date of publication at Zenodo (https://doi.org/10.5281/zenodo.13350229).
- Code to replicate the analyses is available at https://doi.org/10.5281/zenodo.13350229.
- Any additional information required to reanalyze the data reported in this paper is available from the lead contact upon request.

REFERENCES

1. Corbett KS, Edwards DK, Leist SR, Abiona OM, Boyoglu-Barnum S, Gillespie RA, Himansu S, Schäfer A, Ziwawo CT, DiPiazza AT, et al. (2020). SARS-CoV-2 mRNA vaccine design enabled by prototype pathogen preparedness. Nature 586, 567–571. 10.1038/s41586-020-2622-0. [PubMed: 32756549]
2. Jackson LA, Anderson EJ, Rouphael NG, Roberts PC, Makhene M, Coler RN, McCullough MP, Chappell JD, Denison MR, Stevens LJ, et al. (2020). An mRNA Vaccine against SARS-CoV-2

- Preliminary Report. N. Engl. J. Med 383, 1920–1931. 10.1056/NEJMoa2022483. [PubMed: 32663912]

3. Mulligan MJ, Lyke KE, Kitchin N, Absalon J, Gurtman A, Lockhart S, Neuzil K, Raabe V, Bailey R, Swanson KA, et al. (2020). Phase I/II study of COVID-19 RNA vaccine BNT162b1 in adults. Nature 586, 589–593. 10.1038/s41586-020-2639-4. [PubMed: 32785213]
4. Laidlaw BJ, and Ellebedy AH (2022). The germinal centre B cell response to SARS-CoV-2. Nat. Rev. Immunol 22, 7–18. 10.1038/s41577-021-00657-1. [PubMed: 34873279]
5. Muecksch F, Wang Z, Cho A, Gaebler C, Ben Tanfous T, DaSilva J, Bednarski E, Ramos V, Zong S, Johnson B, et al. (2022). Increased memory B cell potency and breadth after a SARS-CoV-2 mRNA boost. Nature 607, 128–134. 10.1038/s41586-022-04778-y. [PubMed: 35447027]
6. Garcia-Beltran WF, St Denis KJ, Hoelzemer A, Lam EC, Nitido AD, Sheehan ML, Berrios C, Ofoman O, Chang CC, Hauser BM, et al. (2022). mRNA-based COVID-19 vaccine boosters induce neutralizing immunity against SARS-CoV-2 Omicron variant. Cell 185, 457–466.e4. 10.1016/j.cell.2021.12.033. [PubMed: 34995482]
7. Carreno JM, Alshammary H, Tcheou J, Singh G, Raskin AJ, Kawabata H, Sominsky LA, Clark JJ, Adelsberg DC, Bielak DA, et al. (2022). Activity of convalescent and vaccine serum against SARS-CoV-2 Omicron. Nature 602, 682–688. 10.1038/s41586-022-04399-5. [PubMed: 35016197]
8. Goel RR, Painter MM, Lundgreen KA, Apostolidis SA, Baxter AE, Giles JR, Mathew D, Pattekar A, Reynaldi A, Khoury DS, et al. (2022). Efficient recall of Omicron-reactive B cell memory after a third dose of SARS-CoV-2 mRNA vaccine. Cell 185, 1875–1887.e8. 10.1016/j.cell.2022.04.009. [PubMed: 35523182]
9. Koutsakos M, and Ellebedy AH (2023). Immunological imprinting: Understanding COVID-19. Immunity 56, 909–913. 10.1016/j.immuni.2023.04.012. [PubMed: 37105169]
10. Buckner CM, Kardava L, El Merhebi O, Narpala SR, Serebryannyy L, Lin BC, Wang W, Zhang X, Lopes de Assis F, Kelly SEM, et al. (2022). Interval between prior SARS-CoV-2 infection and booster vaccination impacts magnitude and quality of antibody and B cell responses. Cell 185, 4333–4346.e14. 10.1016/j.cell.2022.09.032. [PubMed: 36257313]
11. Reynolds CJ, Pade C, Gibbons JM, Otter AD, Lin KM, Muñoz Sandoval D, Pieper FP, Butler DK, Liu S, Joy G, et al. (2022). Immune boosting by B.1.1.529 (Omicron) depends on previous SARS-CoV-2 exposure. Science 377, eabq1841. 10.1126/science.abq1841. [PubMed: 35699621]
12. Johnston TS, Li SH, Painter MM, Atkinson RK, Douek NR, Reeg DB, Douek DC, Wherry EJ, and Hensley SE (2024). Immunological imprinting shapes the specificity of human antibody responses against SARS-CoV-2 variants. Immunity 57, 912–925.e4. 10.1016/j.immuni.2024.02.017. [PubMed: 38490198]
13. Liang CY, Raju S, Liu Z, Li Y, Asthagiri Arunkumar G, Case JB, Scheaffer SM, Zost SJ, Acreman CM, Gagne M, et al. (2024). Imprinting of serum neutralizing antibodies by Wuhan-1 mRNA vaccines. Nature 630, 950–960. 10.1038/s41586-024-07539-1. [PubMed: 38749479]
14. Yisimayi A, Song W, Wang J, Jian F, Yu Y, Chen X, Xu Y, Yang S, Niu X, Xiao T, et al. (2024). Repeated Omicron exposures override ancestral SARS-CoV-2 immune imprinting. Nature 625, 148–156. 10.1038/s41586-023-06753-7. [PubMed: 37993710]
15. Sokal A, Barba-Spaeth G, Hunault L, Fernández I, Broketa M, Meola A, Fourati S, Azzaoui I, Vandenberghe A, Lagouge-Roussey P, et al. (2023). SARS-CoV-2 Omicron BA.1 breakthrough infection drives late remodeling of the memory B cell repertoire in vaccinated individuals. Immunity 56, 2137–2151.e7. 10.1016/j.immuni.2023.07.007. [PubMed: 37543032]
16. Alsoussi WB, Malladi SK, Zhou JQ, Liu Z, Ying B, Kim W, Schmitz AJ, Lei T, Horvath SC, Sturtz AJ, et al. (2023). SARS-CoV-2 Omicron boosting induces de novo B cell response in humans. Nature 617, 592–598. 10.1038/s41586-023-06025-4. [PubMed: 37011668]
17. McGrath JJC, Li L, and Wilson PC (2022). Memory B cell diversity: insights for optimized vaccine design. Trends Immunol. 43, 343–354. 10.1016/j.it.2022.03.005. [PubMed: 35393268]
18. Henry B, and Laidlaw BJ (2023). Functional heterogeneity in the memory B-cell response. Curr. Opin. Immunol 80, 102281. 10.1016/j.coi.2022.102281. [PubMed: 36652774]
19. Glass DR, Tsai AG, Oliveria JP, Hartmann FJ, Kimmey SC, Calderon AA, Borges L, Glass MC, Wagar LE, Davis MM, and Bendall SC (2020). An Integrated Multi-omic Single-Cell Atlas

of Human B Cell Identity. Immunity 53, 217–232.e5. 10.1016/j.immuni.2020.06.013. [PubMed: 32668225]

20. Weisel NM, Joachim SM, Smita S, Callahan D, Elsner RA, Conter LJ, Chikina M, Farber DL, Weisel FJ, and Shlomchik MJ (2022). Surface phenotypes of naive and memory B cells in mouse and human tissues. Nat. Immunol 23, 135–145. 10.1038/s41590-021-01078-x. [PubMed: 34937918]
21. Sokal A, Chappert P, Barba-Spaeth G, Roeser A, Fourati S, Azzaoui I, Vandenberghe A, Fernandez I, Meola A, Bouvier-Alias M, et al. (2021). Maturation and persistence of the anti-SARS-CoV-2 memory B cell response. Cell 184, 1201–1213.e14. 10.1016/j.cell.2021.01.050. [PubMed: 33571429]
22. Rodda LB, Netland J, Shehata L, Pruner KB, Morawski PA, Thouvenel CD, Takehara KK, Eggenberger J, Hemann EA, Waterman HR, et al. (2021). Functional SARS-CoV-2-Specific Immune Memory Persists after Mild COVID-19. Cell 184, 169–183.e17. 10.1016/j.cell.2020.11.029. [PubMed: 33296701]
23. Rodda LB, Morawski PA, Pruner KB, Fahning ML, Howard CA, Franko N, Logue J, Eggenberger J, Stokes C, Golez I, et al. (2022). Imprinted SARS-CoV-2-specific memory lymphocytes define hybrid immunity. Cell 185, 1588–1601.e14. 10.1016/j.cell.2022.03.018. [PubMed: 35413241]
24. Pape KA, Dileepan T, Kabage AJ, Kozysa D, Batres R, Evert C, Matson M, Lopez S, Krueger PD, Graiziger C, et al. (2021). High-affinity memory B cells induced by SARS-CoV-2 infection produce more plasmablasts and atypical memory B cells than those primed by mRNA vaccines. Cell Rep. 37, 109823. 10.1016/j.celrep.2021.109823. [PubMed: 34610291]
25. Goel RR, Apostolidis SA, Painter MM, Mathew D, Pattekar A, Kuthuru O, Gouma S, Hicks P, Meng W, Rosenfeld AM, et al. (2021). Distinct antibody and memory B cell responses in SARS-CoV-2 naive and recovered individuals following mRNA vaccination. Sci. Immunol 6, eabi6950. 10.1126/sciimmunol.abi6950. [PubMed: 33858945]
26. Barateau V, Peyrot L, Saade C, Pozzetto B, Brengel-Pesce K, Elsensohn MH, Allatif O, Guibert N, Compagnon C, Mariano N, et al. (2023). Prior SARS-CoV-2 infection enhances and reshapes spike protein-specific memory induced by vaccination. Sci. Transl. Med 15, eade0550. 10.1126/scitranslmed.ade0550. [PubMed: 36921035]
27. Zurbuchen Y, Michler J, Taeschler P, Adamo S, Cervia C, Raeber ME, Acar IE, Nilsson J, Warnatz K, Soyka MB, et al. (2023). Human memory B cells show plasticity and adopt multiple fates upon recall response to SARS-CoV-2. Nat. Immunol 24, 955–965. 10.1038/s41590-023-01497-y. [PubMed: 37106039]
28. Kardava L, Rachmaninoff N, Lau WW, Buckner CM, Trihemasava K, Blazkova J, Lopes de Assis F, Wang W, Zhang X, Wang Y, et al. (2022). Early human B cell signatures of the primary antibody response to mRNA vaccination. Proc. Natl. Acad. Sci. USA 119, e2204607119. 10.1073/pnas.2204607119. [PubMed: 35759653]
29. Srivastava K, Carreno JM, Gleason C, Monahan B, Singh G, Abbad A, Tcheou J, Raskin A, Kleiner G, van Bakel H, et al. (2024). SARS-CoV-2-infection- and vaccine-induced antibody responses are long lasting with an initial waning phase followed by a stabilization phase. Immunity 57, 587–599 e584. 10.1016/j.immuni.2024.01.017. [PubMed: 38395697]
30. Dugan HL, Stamper CT, Li L, Changrob S, Asby NW, Halfmann PJ, Zheng NY, Huang M, Shaw DG, Cobb MS, et al. (2021). Profiling B cell immunodominance after SARS-CoV-2 infection reveals antibody evolution to non-neutralizing viral targets. Immunity 54, 1290–1303.e7. 10.1016/j.immuni.2021.05.001. [PubMed: 34022127]
31. Matsumoto R, Gray J, Rybkina K, Oppenheimer H, Levy L, Friedman LM, Khamaisi M, Meng W, Rosenfeld AM, Guyer RS, et al. (2023). Induction of bronchus-associated lymphoid tissue is an early life adaptation for promoting human B cell immunity. Nat. Immunol 24, 1370–1381. 10.1038/s41590-023-01557-3. [PubMed: 37460638]
32. Bendall SC, Davis KL, Amir EAD, Tadmor MD, Simonds EF, Chen TJ, Shenfeld DK, Nolan GP, and Pe'er D (2014). Single-cell trajectory detection uncovers progression and regulatory coordination in human B cell development. Cell 157, 714–725. 10.1016/j.cell.2014.04.005. [PubMed: 24766814]

33. Sims GP, Ettinger R, Shirota Y, Yarboro CH, Illei GG, and Lipsky PE (2005). Identification and characterization of circulating human transitional B cells. Blood 105, 4390–4398. 10.1182/blood-2004-11-4284. [PubMed: 15701725]
34. Bohnhorst JO, Bjorgan MB, Thoen JE, Natvig JB, and Thompson KM (2001). Bm1-Bm5 classification of peripheral blood B cells reveals circulating germinal center founder cells in healthy individuals and disturbance in the B cell subpopulations in patients with primary Sjogren's syndrome. J. Immunol 167, 3610–3618. 10.4049/jimmunol.167.7.3610. [PubMed: 11564773]
35. Austin JW, Buckner CM, Kardava L, Wang W, Zhang X, Melson VA, Swanson RG, Martins AJ, Zhou JQ, Hoehn KB, et al. (2019). Overexpression of T-bet in HIV infection is associated with accumulation of B cells outside germinal centers and poor affinity maturation. Sci. Transl. Med 11, eaax0904. 10.1126/scitranslmed.aax0904. [PubMed: 31776286]
36. Conter LJ, Song E, Shlomchik MJ, and Tomayko MM (2014). CD73 expression is dynamically regulated in the germinal center and bone marrow plasma cells are diminished in its absence. PLoS One 9, e92009. 10.1371/journal.pone.0092009. [PubMed: 24664100]
37. Wang X, Rodda LB, Bannard O, and Cyster JG (2014). Integrin-mediated interactions between B cells and follicular dendritic cells influence germinal center B cell fitness. J. Immunol 192, 4601–4609. 10.4049/jimmunol.1400090. [PubMed: 24740506]
38. Huang CQ, Vishwanath S, Carnell GW, Chan ACY, and Heeney JL (2023). Immune imprinting and next-generation coronavirus vaccines. Nat. Microbiol 8, 1971–1985. 10.1038/s41564-023-01505-9. [PubMed: 37932355]
39. Goel RR, Painter MM, Apostolidis SA, Mathew D, Meng W, Rosenfeld AM, Lundgreen KA, Reynaldi A, Khoury DS, Pattekar A, et al. (2021). mRNA vaccines induce durable immune memory to SARS-CoV-2 and variants of concern. Science 374, abm0829. 10.1126/science.abm0829. [PubMed: 34648302]
40. Painter MM, Johnston TS, Lundgreen KA, Santos JJS, Qin JS, Goel RR, Apostolidis SA, Mathew D, Fulmer B, Williams JC, et al. (2023). Prior vaccination promotes early activation of memory T cells and enhances immune responses during SARS-CoV-2 breakthrough infection. Nat. Immunol 24, 1711–1724. 10.1038/s41590-023-01613-y. [PubMed: 37735592]
41. Andrews SF, Chambers MJ, Schramm CA, Plyler J, Raab JE, Kanekiyo M, Gillespie RA, Ransier A, Darko S, Hu J, et al. (2019). Activation Dynamics and Immunoglobulin Evolution of Pre-existing and Newly Generated Human Memory B cell Responses to Influenza Hemagglutinin. Immunity 51, 398–410.e5. 10.1016/j.immuni.2019.06.024. [PubMed: 31350180]
42. Kotaki R, Adachi Y, Moriyama S, Onodera T, Fukushi S, Nagakura T, Tonouchi K, Terahara K, Sun L, Takano T, et al. (2022). SARS-CoV-2 Omicron-neutralizing memory B cells are elicited by two doses of BNT162b2 mRNA vaccine. Sci. Immunol 7, eabn8590. 10.1126/sciimmunol.abn8590. [PubMed: 35113654]
43. Wec AZ, Haslwanter D, Abdiche YN, Shehata L, Pedreño-Lopez N, Moyer CL, Bornholdt ZA, Lilov A, Nett JH, Jangra RK, et al. (2020). Longitudinal dynamics of the human B cell response to the yellow fever 17D vaccine. Proc. Natl. Acad. Sci. USA 117, 6675–6685. 10.1073/pnas.1921388117. [PubMed: 32152119]
44. Fels JM, Maurer DP, Herbert AS, Wirchnianski AS, Vergnolle O, Cross RW, Abelson DM, Moyer CL, Mishra AK, Aguilan JT, et al. (2021). Protective neutralizing antibodies from human survivors of Crimean-Congo hemorrhagic fever. Cell 184, 3486–3501.e21. 10.1016/j.cell.2021.05.001. [PubMed: 34077751]
45. Nellore A, Zumaquero E, Scharer CD, Fucile CF, Tipton CM, King RG, Mi T, Mousseau B, Bradley JE, Zhou F, et al. (2023). A transcriptionally distinct subset of influenza-specific effector memory B cells predicts long-lived antibody responses to vaccination in humans. Immunity 56, 847–863.e8. 10.1016/j.immuni.2023.03.001. [PubMed: 36958335]
46. Lam N, Lee Y, and Farber DL (2024). A guide to adaptive immune memory. Nat. Rev. Immunol 24, 810–829. 10.1038/s41577-024-01040-6. [PubMed: 38831162]
47. Burton AR, and Maini MK (2021). Human antiviral B cell responses: Emerging lessons from hepatitis B and COVID-19. Immunol. Rev 299, 108–117. 10.1111/imr.12953. [PubMed: 33559128]

48. Goldblatt D, Alter G, Crotty S, and Plotkin SA (2022). Correlates of protection against SARS-CoV-2 infection and COVID-19 disease. Immunol. Rev 310, 6–26. 10.1111/imr.13091. [PubMed: 35661178]
49. Tang J, Zeng C, Cox TM, Li C, Son YM, Cheon IS, Wu Y, Behl S, Taylor JJ, Chakaraborty R, et al. (2022). Respiratory mucosal immunity against SARS-CoV-2 after mRNA vaccination. Sci. Immunol 7, eadd4853. 10.1126/sciimmunol.add4853. [PubMed: 35857583]
50. Moon KR, van Dijk D, Wang Z, Gigante S, Burkhardt DB, Chen WS, Yim K, Elzen AVD, Hirn MJ, Coifman RR, et al. (2019). Visualizing structure and transitions in high-dimensional biological data. Nat. Biotechnol 37, 1482–1492. 10.1038/s41587-019-0336-3. [PubMed: 31796933]
51. Setty M, Tadmor MD, Reich-Zeliger S, Angel O, Salame TM, Kathail P, Choi K, Bendall S, Friedman N, and Pe'er D (2016). Wishbone identifies bifurcating developmental trajectories from single-cell data. Nat. Biotechnol 34, 637–645. 10.1038/nbt.3569. [PubMed: 27136076]
52. Pajon R, Doria-Rose NA, Shen X, Schmidt SD, O'Dell S, McDanal C, Feng W, Tong J, Eaton A, Maglinao M, et al. (2022). SARS-CoV-2 Omicron Variant Neutralization after mRNA-1273 Booster Vaccination. N. Engl. J. Med 386, 1088–1091. 10.1056/NEJMc2119912. [PubMed: 35081298]
53. Chalkias S, Whatley JL, Eder F, Essink B, Khetan S, Bradley P, Brosz A, McGhee N, Tomassini JE, Chen X, et al. (2023). Original SARS-CoV-2 monovalent and Omicron BA.4/BA.5 bivalent COVID-19 mRNA vaccines: phase 2/3 trial interim results. Nat. Med 29, 2325–2333. 10.1038/s41591-023-02517-y. [PubMed: 37653342]
54. Good-Jacobson KL (2018). Strength in diversity: Phenotypic, functional, and molecular heterogeneity within the memory B cell repertoire. Immunol. Rev 284, 67–78. 10.1111/imr.12663. [PubMed: 29944763]
55. Cancro MP, and Tomayko MM (2021). Memory B cells and plasma cells: The differentiative continuum of humoral immunity. Immunol. Rev 303, 72–82. 10.1111/imr.13016. [PubMed: 34396546]
56. Weisel F, and Shlomchik M (2017). Memory B Cells of Mice and Humans. Annu. Rev. Immunol 35, 255–284. 10.1146/annurev-immunol-041015-055531. [PubMed: 28142324]
57. Chappert P, Huetz F, Espinasse MA, Chatonnet F, Pannetier L, Da Silva L, Goetz C, Mégret J, Sokal A, Crickx E, et al. (2022). Human anti-smallpox long-lived memory B cells are defined by dynamic interactions in the splenic niche and long-lasting germinal center imprinting. Immunity 55, 1872–1890.e9. 10.1016/j.immuni.2022.08.019. [PubMed: 36130603]
58. Davis-Porada J, George AB, Lam N, Caron DP, Gray JI, Huang J, Hwu J, Wells SB, Matsumoto R, Kubota M, et al. (2024). Maintenance and functional regulation of immune memory to COVID-19 vaccines in tissues. Immunity 57, 2895–2913.e8. 10.1016/j.immuni.2024.10.003. [PubMed: 39510068]
59. Zhong Y, Kang AYH, Tay CJX, Li HE, Elyana N, Tan CW, Yap WC, Lim JME, Le Bert N, Chan KR, et al. (2024). Correlates of protection against symptomatic SARS-CoV-2 in vaccinated children. Nat. Med 30, 1373–1383. 10.1038/s41591-024-02962-3. [PubMed: 38689059]
60. Xu Q, Milanez-Almeida P, Martins AJ, Radtke AJ, Hoehn KB, Oguz C, Chen J, Liu C, Tang J, Grubbs G, et al. (2023). Adaptive immune responses to SARS-CoV-2 persist in the pharyngeal lymphoid tissue of children. Nat. Immunol 24, 186–199. 10.1038/s41590-022-01367-z. [PubMed: 36536106]
61. Turner JS, O'Halloran JA, Kalaidina E, Kim W, Schmitz AJ, Zhou JQ, Lei T, Thapa M, Chen RE, Case JB, et al. (2021). SARS-CoV-2 mRNA vaccines induce persistent human germinal centre responses. Nature 596, 109–113. 10.1038/s41586-021-03738-2. [PubMed: 34182569]
62. Rathmell JC, Townsend SE, Xu JC, Flavell RA, and Goodnow CC (1996). Expansion or elimination of B cells in vivo: dual roles for CD40- and Fas (CD95)-ligands modulated by the B cell antigen receptor. Cell 87, 319–329. 10.1016/s0092-8674(00)81349-5. [PubMed: 8861915]
63. Ellebedy AH, Jackson KJL, Kissick HT, Nakaya HI, Davis CW, Roskin KM, McElroy AK, Oshansky CM, Elbein R, Thomas S, et al. (2016). Defining antigen-specific plasmablast and memory B cell subsets in human blood after viral infection or vaccination. Nat. Immunol 17, 1226–1234. 10.1038/ni.3533. [PubMed: 27525369]

64. Gilbert PB, Donis RO, Koup RA, Fong Y, Plotkin SA, and Follmann D (2022). A Covid-19 Milestone Attained - A Correlate of Protection for Vaccines. N. Engl. J. Med 387, 2203–2206. 10.1056/NEJMp2211314. [PubMed: 36507702]

65. Holla P, Dizon B, Ambegaonkar AA, Rogel N, Goldschmidt E, Boddapati AK, Sohn H, Sturdevant D, Austin JW, Kardava L, et al. (2021). Shared transcriptional profiles of atypical B cells suggest common drivers of expansion and function in malaria, HIV, and autoimmunity. Sci. Adv 7, eabg8384. 10.1126/sciadv.abg8384. [PubMed: 34039612]

66. Moir S, and Fauci AS (2017). B-cell responses to HIV infection. Immunol. Rev 275, 33–48. 10.1111/imr.12502. [PubMed: 28133792]

67. Andreano E, Paciello I, Piccini G, Manganaro N, Pileri P, Hyseni I, Leonardi M, Pantano E, Abbiento V, Benincasa L, et al. (2021). Hybrid immunity improves B cells and antibodies against SARS-CoV-2 variants. Nature 600, 530–535. 10.1038/s41586-021-04117-7. [PubMed: 34670266]

68. Havervall S, Marking U, Svensson J, Greilert-Norin N, Bacchus P, Nilsson P, Hober S, Gordon M, Blom K, Klingström J, et al. (2022). Anti-Spike Mucosal IgA Protection against SARS-CoV-2 Omicron Infection. N. Engl. J. Med 387, 1333–1336. 10.1056/NEJMc2209651. [PubMed: 36103621]

69. Purtha WE, Tedder TF, Johnson S, Bhattacharya D, and Diamond MS (2011). Memory B cells, but not long-lived plasma cells, possess antigen specificities for viral escape mutants. J. Exp. Med 208, 2599–2606. 10.1084/jem.20110740. [PubMed: 22162833]

70. Irrgang P, Gerling J, Kocher K, Lapuente D, Steininger P, Habenicht K, Wytopil M, Beileke S, Schäfer S, Zhong J, et al. (2023). Class switch toward noninflammatory, spike-specific IgG4 antibodies after repeated SARS-CoV-2 mRNA vaccination. Sci. Immunol 8, eade2798. 10.1126/sciimmunol.ade2798. [PubMed: 36548397]

71. Akhtar M, Islam MR, Khaton F, Soltana UH, Jafrin SA, Rahman SIA, Tauheed I, Ahmed T, Khan II, Akter A, et al. (2023). Appearance of tolerance-induction and non-inflammatory SARS-CoV-2 spike-specific IgG4 antibodies after COVID-19 booster vaccinations. Front. Immunol 14, 1309997. 10.3389/fimmu.2023.1309997. [PubMed: 38173725]

72. Hartley GE, Fryer HA, Gill PA, Boo I, Bornheimer SJ, Hogarth PM, Drummer HE, O'Hehir RE, Edwards ESJ, and van Zelm MC (2024). Homologous but not heterologous COVID-19 vaccine booster elicits IgG4+ B-cells and enhanced Omicron subvariant binding. NPJ Vaccines 9, 129. 10.1038/s41541-024-00919-8. [PubMed: 39013889]

73. Teng IT, Nazzari AF, Choe M, Liu T, Oliveira de Souza M, Petrova Y, Tsybovsky Y, Wang S, Zhang B, Artamonov M, et al. (2022). Molecular probes of spike ectodomain and its subdomains for SARS-CoV-2 variants, Alpha through Omicron. PLoS One 17, e0268767. 10.1371/journal.pone.0268767. [PubMed: 35609088]

74. Naldini L, Blömer U, Gage FH, Trono D, and Verma IM (1996). Efficient transfer, integration, and sustained long-term expression of the transgene in adult rat brains injected with a lentiviral vector. Proc. Natl. Acad. Sci. USA 93, 11382–11388. 10.1073/pnas.93.21.11382. [PubMed: 8876144]

75. Corbett KS, Gagne M, Wagner DA, O' Connell S, Narpala SR, Flebbe DR, Andrew SF, Davis RL, Flynn B, Johnston TS, et al. (2021). Protection against SARS-CoV-2 Beta variant in mRNA-1273 vaccine-boosted nonhuman primates. Science 374, 1343–1353. 10.1126/science.abl8912. [PubMed: 34672695]

76. Ober Shepherd BL, Scott PT, Hutter JN, Lee C, McCauley MD, Guzman I, Bryant C, McGuire S, Kennedy J, Chen WH, et al. (2024). SARS-CoV-2 recombinant spike ferritin nanoparticle vaccine adjuvanted with Army Liposome Formulation containing monophosphoryl lipid A and QS-21: a phase 1, randomised, double-blind, placebo-controlled, first-in-human clinical trial. Lancet. Microbe 5, e581–e593. 10.1016/S2666-5247(23)00410-X. [PubMed: 38761816]

77. Gagne M, Moliva JI, Foulds KE, Andrew SF, Flynn BJ, Werner AP, Wagner DA, Teng IT, Lin BC, Moore C, et al. (2022). mRNA-1273 or mRNA-Omicron boost in vaccinated macaques elicits similar B cell expansion, neutralizing responses, and protection from Omicron. Cell 185, 1556–1571.e18. 10.1016/j.cell.2022.03.038. [PubMed: 35447072]

78. Hothorn T, Hornik K, Wiel M.A.v.d., and Zeileis A (2008). Implementing a Class of Permutation Tests: The coin Package. J. Stat. Softw 28, 1–23. 10.18637/jss.v028.i08. [PubMed: 27774042]

79. Cribari-Neto F, and Zeileis A (2010). Beta Regression in R. J. Stat. Softw 34, 1–24. 10.18637/jss.v034.i02.

80. Grün B, Kosmidis I, and Zeileis A (2012). Extended Beta Regression in R: Shaken, Stirred, Mixed, and Partitioned. J. Stat. Software 48, 1–25. 10.18637/jss.v048.i11.

Highlights

- COVID-19 mRNA booster vaccine elicits spike^{+} antibody and B cell responses without infection
- Magnitude of response is similar between infection and first booster dose without infection
- More IgG/CD71^{+} and IgA with infection versus IgG/CD27^{-} with vaccination among spike^{+} B cells
- CD73+ and CD73^{-} memory and GC-like B cells contribute to immunity irrespective of exposure

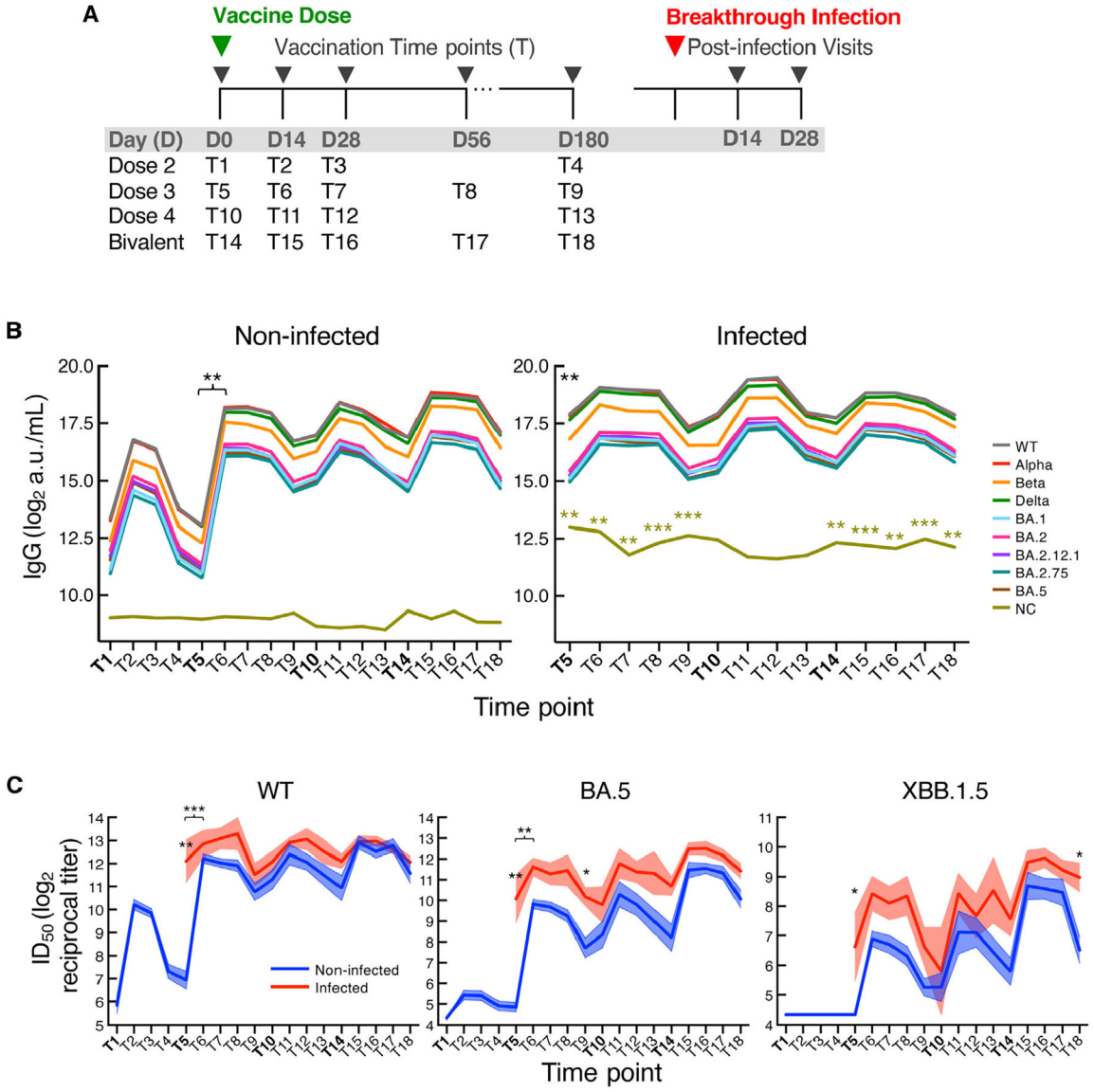

Figure 1. Similar antibody responses with and without prior infection after booster vaccine

(A) The cohort and vaccination/blood draw schedule. T4 is 180 days after dose 1.

(B) Mean IgG RBD and NC binding titers expressed as a.u./mL serum.

(C) Mean ± SEM serum neutralizing titers against SARS-CoV-2 lentiviral pseudovirus expressed as reciprocal ID_{50}.

Statistical analyses by permutation test. *FDR ≤ 0.05, **FDR ≤ 0.01 and ***FDR ≤ 0.001; comparing non-infected to infected at a single time point without a bracket and slopes between the indicated time points with a bracket. Black asterisks ** in (B) represent FDR values for all nine RBD antigens. Bold time points indicate day 0 of vaccine dose. See also Figure S1 and Table S1.

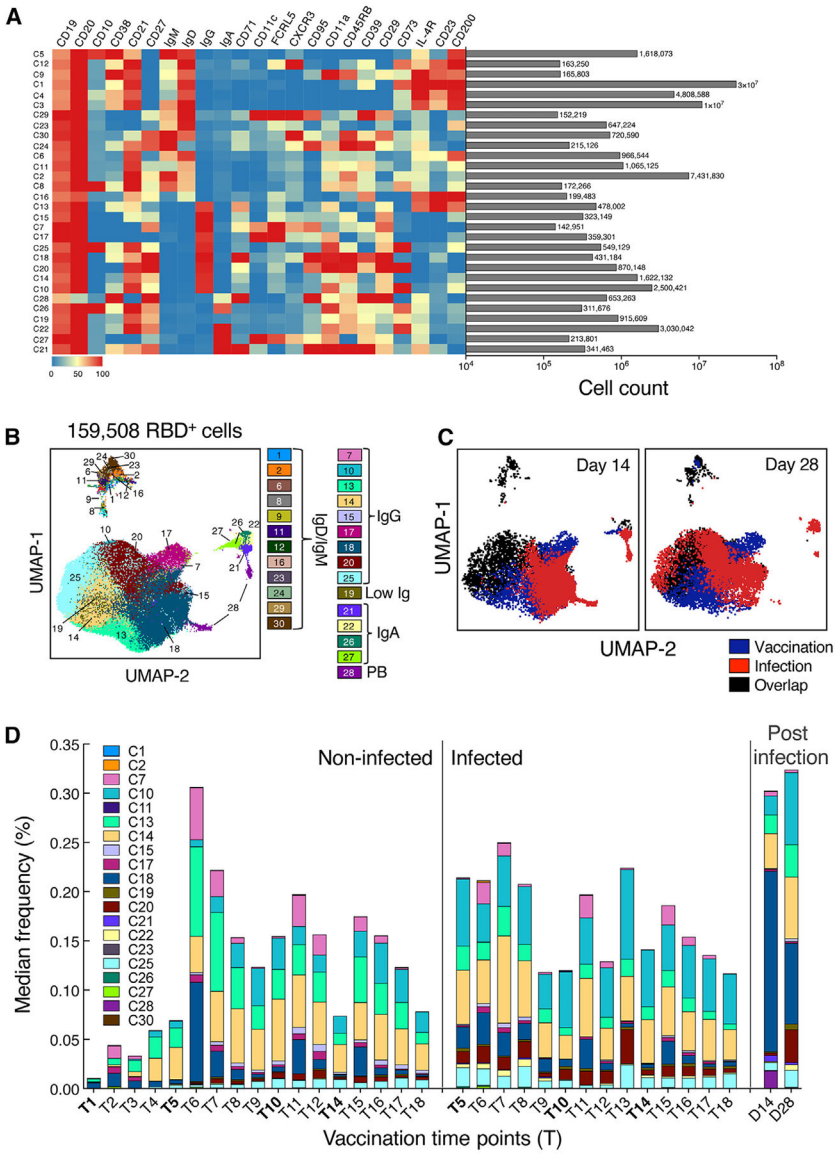

Figure 2. Different RBD-reactive clusters fluctuate post vaccination and post infection

(A) Heatmap of unsupervised clustering performed with 23 B cell markers, showing the number of cells in each cluster.

(B) UMAP of RBD-reactive clusters.

(C) UMAP in (B) overlayed by colors, showing RBD reactivity on days 14 and 28 post vaccination or post infection alone or their overlap.

(D) Median RBD reactivities in each cluster at each time point post vaccination or post infection (days 14 and 28) as a percentage of total $CD19^+$ B cells. Bold time points indicate day 0 of the vaccine dose. See also Figure S2 and Table S3.

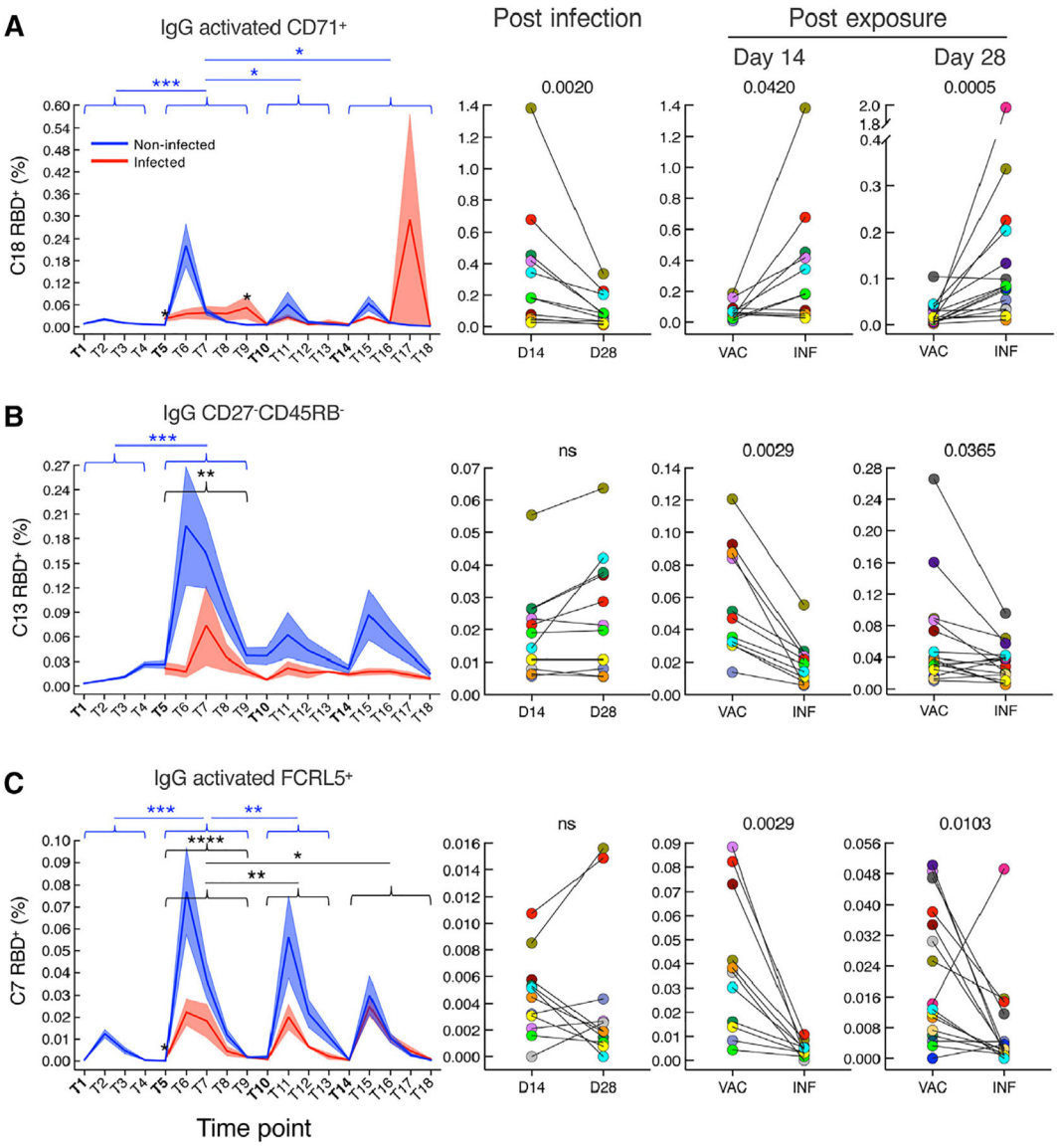

Figure 3. RBD reactivities in activated clusters fluctuate differently post vaccination versus post infection

(A) C18 RBD reactivity across time points and paired time points comparing days 14 and 28 post infection (INF) and corresponding post-vaccination (VAC) alone.

(B) As in (A) for C13.

(C) As in (A) for C7.

Cluster RBD reactivity percentages are of total $CD19^+$ B cells. Data across all time points represent mean ± SEM. Statistical analyses by general linear model (GLM) across time points and by paired Wilcoxon test for paired time points. *FDR ≤ 0.05, **FDR ≤ 0.01, ***FDR ≤ 0.001, and ****FDR ≤ 0.0001 or exact FDR values above graphs; comparing non-infected to infected at single time points without a bracket and peak or AUC within a dose with a bracket and across doses with connecting lines; blue comparing within non-infected and black comparing infected to non-infected; ns, not significant. Bold time points indicate day 0 of vaccine dose. See also Figure S3.

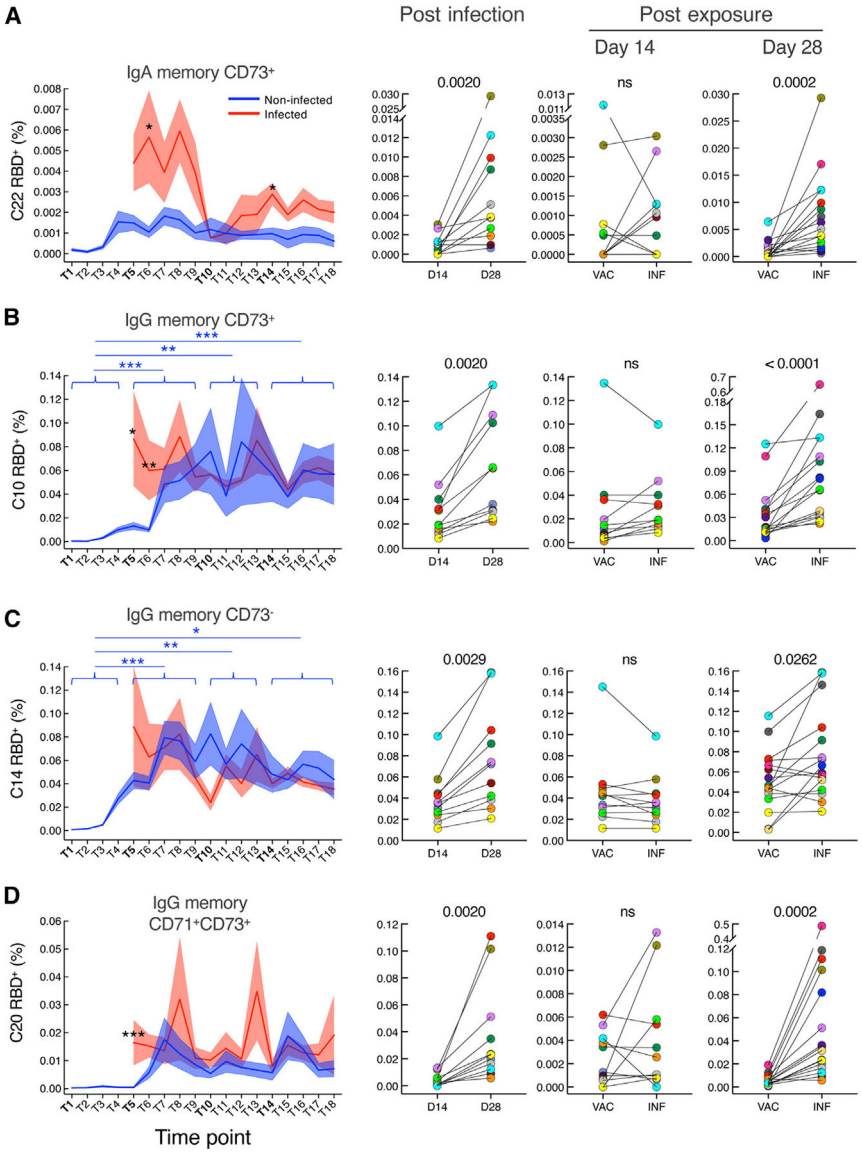

Figure 4. Similar RBD reactivities in memory clusters after booster vaccine

(A) C22 RBD reactivity across time points and paired time points comparing days 14 and 28 post infection (INF) and corresponding post vaccination (VAC) alone.

(B) As in (A) for C10.

(C) As in (A) for C14.

(D) As in (A) for C20.

Cluster RBD reactivity percentages are of total $CD19^+$ B cells. Data across all time points represent mean ± SEM. Statistical analyses by GLM across time points and by paired Wilcoxon test for paired time points. *FDR ≤ 0.05, ***FDR ≤ 0.001, and ****FDR ≤ 0.0001 or exact FDR values above graphs; comparing non-infected to infected at single time points without a bracket and peak or AUC within a dose with a bracket and across doses with connecting lines; blue comparing within non-infected and black comparing infected to non-infected. Bold time points indicate day 0 of vaccine dose. See also Figure S4.

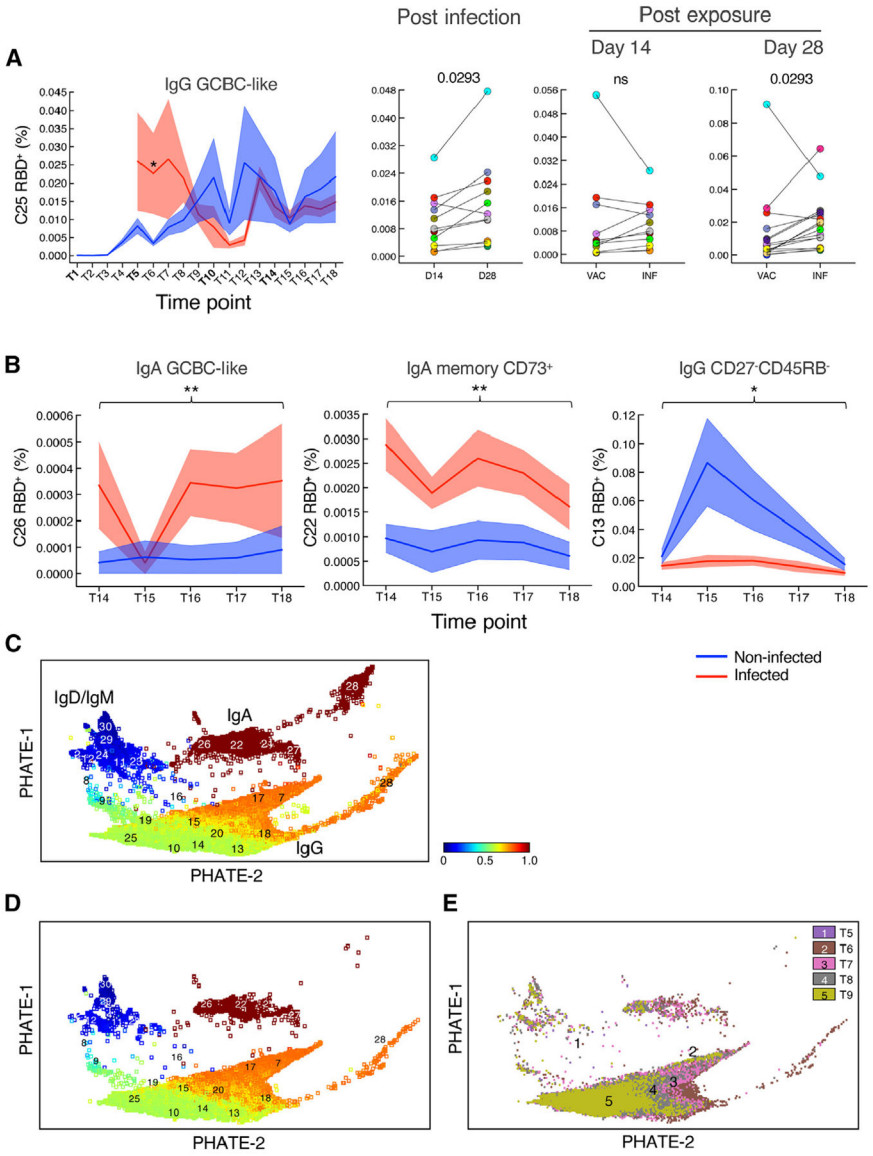

Figure 5. GCBC core contributors to RBD responses post vaccination

(A) C25 RBD reactivity across time points and paired time points comparing days 14 and 8 post infection (INF) and corresponding post vaccination (VAC) alone. Bold time points indicate day ay 0 of vaccine dose.

(B) C26, C22, and C13 RBD reactivities at baseline and time points after bivalent vaccination after removing four individuals infected during this period.

(C) PHATE mapping in pseudo-time of all time points.

(D) PHATE mapping in pseudo-time of non-infected RBD-reactive clusters T5–T9 (dose 3).

(E) As in (D) in real time.

Cluster RBD reactivity percentages are of total $CD19^+$ B cells. Data across all time points represent mean ± SEM. Statistical analyses by GLM across time points and by paired Wilcoxon test for paired time points. *FDR ≤ 0.05, **FDR ≤ 0.01 comparing single time

points (A) or AUC within-dose time points (B) between infected and non-infected or exact FDR values above graphs. See also Figure S5.

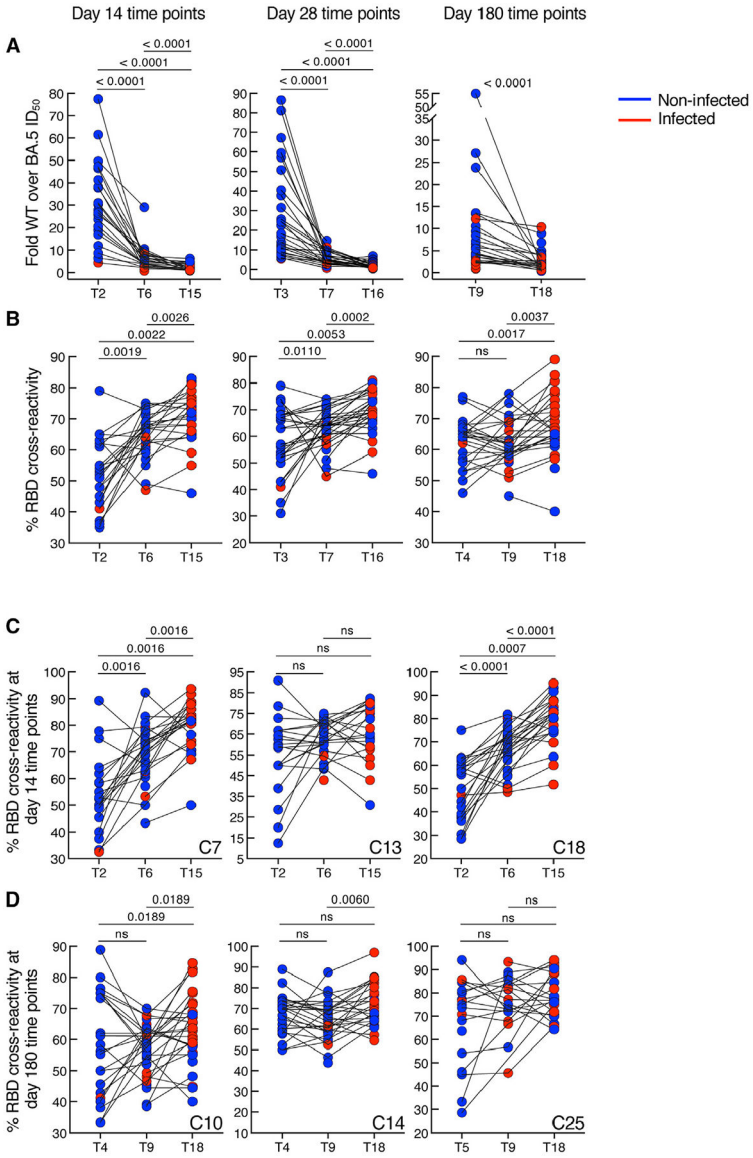

Figure 6. Cross-reactive RBD neutralizing antibodies and B cells modulated by exposures

(A) WT over BA.5 fold differences in ID_{50} neutralizing titers comparing doses 2, 3, and bivalent on days 14 and 28 and doses 3 and bivalent on day 180.

(B) $WT^+/BA.4/5^+$ over WT^+ RBD reactivities for all clusters combined comparing doses 2, 3, and bivalent on days 14, 28, and 180.

(C) $WT^+/BA.4/5^+$ over WT^+ RBD reactivities of activated C7, C13, and C18 clusters, comparing doses 2, 3, and bivalent on day 14.

(D) $WT^+/BA.4/5^+$ over WT^+ RBD reactivities as in (C) of memory C10 and C14 and GCBC C25 clusters, comparing doses 2, 3, and bivalent on day 180.

Statistical analyses by Wilcoxon signed-rank test with Benjamini-Hochberg correction for three-way testing. *p* values are shown above graphs. Non-infected time points are shown in blue and infected time points in red. See also Figure S6.

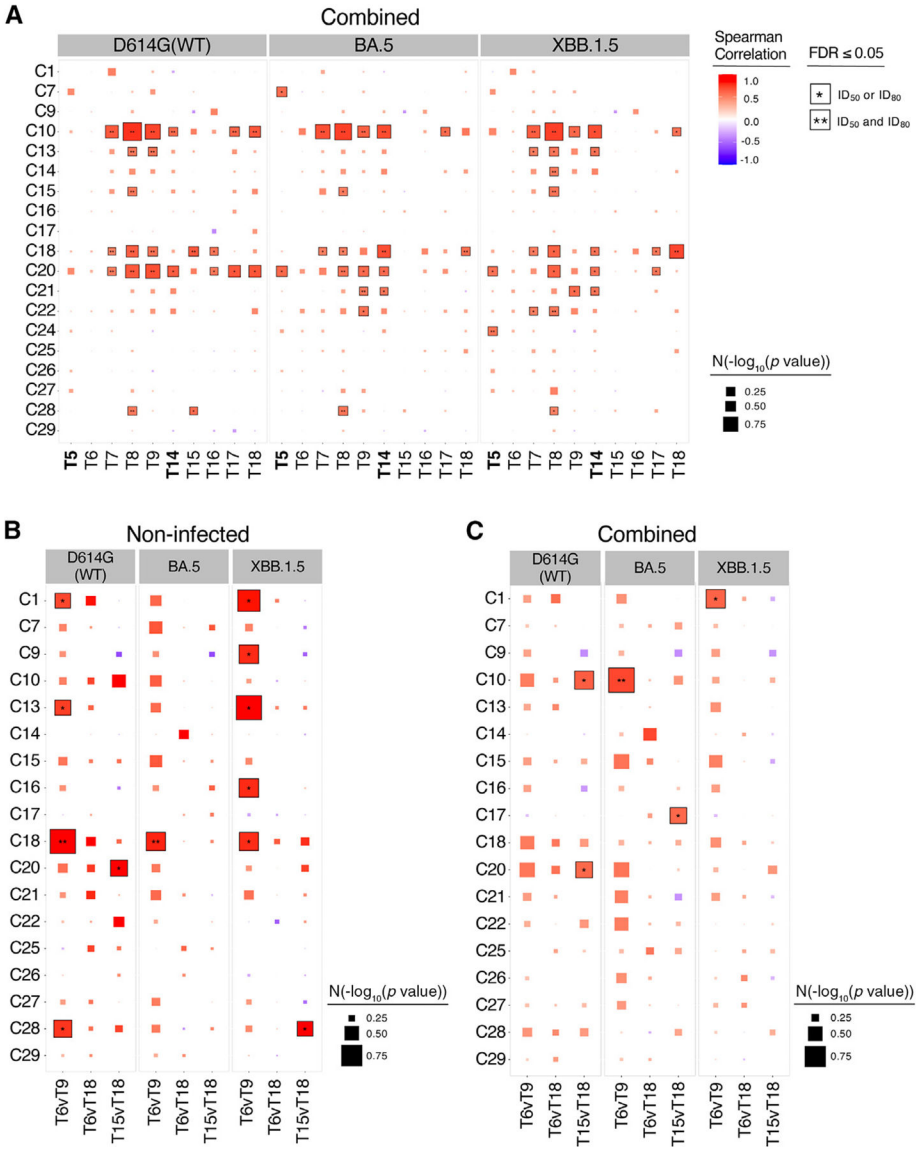

Figure 7. Several RBD-reactive clusters correlate with neutralizing antibody titers at concurrent and non-concurrent time points and strongest in the absence of prior infection

(A) Combined non-infected and infected correlations at concurrent time points. Bold time points indicate day 0 of vaccine dose.

(B) Non-infected correlations at non-concurrent time points: T6 or T15 for RBD-reactive clusters and T9 or T18 for neutralizing antibodies.

(C) As in (B) for combined non-infected and infected data. Cluster RBD reactivity percentages are of total $CD19^+$ B cells.

Statistics by Spearman rank correlation and corrected for multiple testing by Benjamini-Hochberg. ID_{50} values are shown when both ID_{50} and ID_{80} were significant. Tile sizes correspond to the normalized (N) significance value calculated as $-\log_{10}(p \text{ value})$, scaled by the maximum $-\log_{10}(p \text{ value})$ and multiplied by 0.9 to restrict the range to [0, 0.9]. See also Figure S7.

KEY RESOURCES TABLE

REAGENT or RESOURCE	SOURCE	IDENTIFIER
Antibodies		
Mouse anti-human CD45 BUV805 (clone HI30)	BD Biosciences	Cat#612891; RRID: AB_2870179
Mouse anti-human CD19 BV650 (Clone SJ25C1)	BD Biosciences	Cat#563226; RRID: AB_2744313
Mouse anti-human CD10 BB515 (Clone HI10a)	BD Biosciences	Cat#564638; RRID: AB_2744267
Mouse anti-human IgG PE-Cy7 (Clone G18-145)	BD Biosciences	Cat#561298; RRID: AB_10611712
Mouse anti-human CD11c BUV395 (clone B-ly6)	BD Biosciences	Cat#563787; RRID: AB_2744274
Mouse anti-human CD45RB BUV496 (clone MT4)	BD Biosciences	Cat#750194; RRID: AB_2874396
Mouse anti-human CD23 BUV563 (clone M-L233)	BD Biosciences	Cat#741389; RRID: AB_2870886
Mouse anti-human CD11a V480 (clone HI111)	BD Biosciences	Cat#746551; RRID: AB_2743841
Mouse anti-human CD200 BV510 (clone MRC OX-104)	BD Biosciences	Cat#563254; RRID: AB_2738099
Mouse anti-human CD124 (IL-4R) BB700 (clone hIL4R-M57)	BD Biosciences	Cat#745925; RRID: AB_2871637
Mouse anti-human CD3 BV570 (Clone UCHT1)	Biolegend	Cat#300436; RRID: AB_2562124
Mouse anti-human IgD BV605 (Clone IA6-2)	Biolegend	Cat#348232; RRID: AB_2563337
Mouse anti-human IgM BV711 (Clone MHM-88)	Biolegend	Cat#314540; RRID: AB_2687215
Mouse anti-human CD27 BV785 (Clone O323)	Biolegend	Cat#302832; RRID: AB_2562674
Mouse anti-human CD21 PE/Dazzle594 (Clone BU32)	Biolegend	Cat#354922; RRID: AB_2750243
Mouse anti-human CXCR3 PE-Fire 640 (clone G025H7)	Biolegend	Cat#353764; RRID: AB_2922569
Mouse anti-human CD39 PE-Fire 810 (clone A1)	Biolegend	Cat#328245; RRID: AB_2894563
Mouse anti-human CD95 PE-Cy5 (clone DX2)	Biolegend	Cat#305610; RRID: AB_314548
Mouse anti-human CD29 Alexa Fluor 647 (clone TS2/16)	Biolegend	Cat#303018; RRID: AB_2130080
Mouse anti-human CD307e (FCRL5) APC (clone 509f6)	Biolegend	Cat#340306; RRID: AB_2564327
Mouse anti-human CD38 APC/Fire810 (clone HB-7)	Biolegend	Cat#356644; RRID: AB_2860936
Mouse anti-human CD71 Alexa Fluor 700 (clone CY1G4)	Biolegend	Cat#334130; RRID: AB_2888770
Mouse anti-human CD73 NovaFluor Yellow 700 (clone AD2)	ThermoFisher	Cat#H016T03Y06; RRID: AB_3098190
Mouse anti-human CD20 APC-Vio 770 (Clone LT20)	Miltenyi Biotec	Cat#130-113-371; RRID: AB_2726419
Mouse anti-human IgA VioBlue (Clone IS11-8E10)	Miltenyi Biotec	Cat#130-113-479; RRID: AB_2726166
Biological samples		
Human peripheral blood samples from SARS-CoV-2 mRNA vaccine recipients	Collected Clinical Center, NIH	Clinical Trial ID: NCT00001281 Clinical Trial ID: NCT05078905
Chemicals, peptides, and recombinant proteins		
Biotinylated SARS-CoV-2 S protein S1	Biolegend	Cat#793806
Biotinylated SARS-CoV-2 Spike RBD	AcroBiosystems	Cat# SPD-C82E9
Biotinylated SARS-CoV-2 Spike RBD (BA.4/5)	AcroBiosystems	Cat#SPD-C82Ew
Biotinylated SARS-CoV-2 S NTD	VRC, NIH[73]	N/A
Biotinylated SARS-CoV-2 S NTD (BA.4/5)	VRC, NIH[73]	N/A
Streptavidin R-Phycoerythrin	ThemoFisher	Cat#S21388
Streptavidin Alexa Fluor 488	ThemoFisher	Cat#S32354
Streptavidin BV421	Biolegend	Cat#405225
Streptavidin BUV615	BD Biosciences	Cat#613013

REAGENT or RESOURCE	SOURCE	IDENTIFIER
Streptavidin BUV737	BD Biosciences	Cat#612775
Zombie NIR Fixable Viability Dye	Biolegend	Cat#423105
Critical commercial assays		
V-PLEX SARS-CoV-2 key variant RBD panel 1 IgG kit	Meso Scale Discovery	Cat#K15659U
V-PLEX SARS-CoV-2 key variant RBD panel 1 IgA kit	Meso Scale Discovery	Cat#K15661U
Deposited data		
Original/source data for all figures and the original codes for statistical analysis	This paper	https://doi.org/10.5281/zenodo.13350229
Experimental models: Cell lines		
HEK-293T/17	ATCC	Cat#CRL-11268; RRID: CVCL_1926
HEK-293T-ACE2	Michael Farzan & Huihui Mu, Scripps Research	N/A
Recombinant DNA		
VRC5601: pHR'CMV Luc	I.M. Verma Naldini et al.[74]	N/A
VRC5602: pCMV DR8.2	I.M. Verma Naldini et al.[74]	N/A
Spike_SARS-CoV-2 D614G	VRC, NIHCorbett et al.[75]	N/A
Spike_SARS-CoV-2 BA.5	VRC, NIHOber Shepherd et al.[76]	N/A
Spike_SARS-CoV-2 XBB.1.5	VRC, NIH Ober Shepherd et al.[76]	N/A
Software and algorithms		
SpectroFlo	Cytek Biosciences	RRID: SCR_025494
FlowJo v10.10	BD Biosciences	RRID: SCR_008520
OMIQ	OMIQ/Dotmatics	N/A
Labkey v19.2	Labkey	N/A
Methodical Mind vS600MM	Meso Scale Discovery	N/A
GraphPad Prism v10.3	GraphPad	RRID: SCR_002798
R v4.3.3	R Project	RRID: SCR_001905